NASA TECHNICAL NOTE

NASA TN D-2455

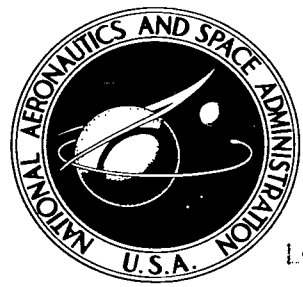

BLAST EFFECTS OF TWIN VARIABLE-CANT ROCKET NOZZLES ON VISIBILITY DURING LANDING ON A PARTICLE-COVERED SURFACE

by George J. Hurt, Jr., and Lindsay J. Lina

Langley Research Center
Langley Station, Hampton, Va.

NATIONAL AERONAUTICS AND SPACE ADMINISTRATION • WASHINGTON, D. C. • DECEMBER 1964

BLAST EFFECTS OF TWIN VARIABLE-CANT ROCKET NOZZLES ON VISIBILITY DURING LANDING ON A PARTICLE-COVERED SURFACE

By George J. Hurt, Jr., and Lindsay J. Lina

Langley Research Center
Langley Station, Hampton, Va.

Technical Film Supplement L-689 available on request.

NATIONAL AERONAUTICS AND SPACE ADMINISTRATION

For sale by the Office of Technical Services, Department of Commerce,
Washington, D.C. 20230 -- Price $1.75

BLAST EFFECTS OF TWIN VARIABLE-CANT ROCKET NOZZLES ON VISIBILITY DURING LANDING ON A PARTICLE-COVERED SURFACE

By George J. Hurt, Jr., and Lindsay J. Lina

SUMMARY

A limited investigation has been conducted to determine the jet-blast effect of twin variable-cant supersonic nozzles. These tests were made to examine the result of using canted main rocket engines to sweep the blast debris outward from the proposed landing area of a rocket-powered vehicle making a vertical approach to a touchdown. Cant angles from 0° to 75°, at intervals of 15°, were tested at low ambient pressure and at atmospheric ambient pressure. Nozzle chamber pressures used were 400 psi and 2000 psi.

Observation of the blast effects in low ambient pressure and in atmospheric-pressure environments indicate that much better visibility might be expected in landing on the moon's surface than a landing under similar circumstances in the earth's atmosphere. Experience with VTOL jet aircraft landing in loose material would then give a pessimistic view of what is to be expected if a jet of equal thrust were used to land on the moon's surface. Simulation of lunar landings with rocket vehicles on earth may possibly give a realistic visibility simulation if nozzle cant angles of about 45° are used on earth to simulate the lunar landing, because the visibility away from the plane of the cant will be about equal to visibility under low atmospheric-pressure conditions. However, visibility into the direction of the cant would be poor and if the vehicle is traveling in that direction, obstacles may not be seen until possibly too late for corrective action to be taken by the pilot.

INTRODUCTION

One concept of a lunar landing is a tail-first vertical descent to the landing area using rocket power for braking. As the vehicle approaches the landing site there is a possibility that material dislodged from the lunar surface by the rocket blast will obscure visibility and perhaps alter the landing site so as to preclude a safe landing. The flying debris may also be a material hazard to the descending vehicle. As little is known about the composition of the lunar surface, steps will have to be taken in designing the landing vehicle to insure maximum visibility during the approach phase. Minimum disturbance of the landing site under the most unfavorable surface conditions may also be a

critical design factor. Studies made of the behavior of debris under such conditions are presented in references 1 to 6.

A possible method of keeping the line of sight to the proposed touchdown point clear and insuring against vehicle damage from blast debris would be to use twin rocket engines canted so that the exhaust gases would tend to sweep the debris outward from the proposed touchdown point. Initial braking would probably be accomplished with the nozzles in the zero cant position. At some predetermined altitude the pilot would cant the nozzles to an optimum angle. Since, at this phase of the approach, the vehicle rate of descent would be comparatively slow, the loss of thrust due to nozzle canting would not be critical. The multiengine configuration of the canted-nozzle design would also afford a possible single-engine abort capability.

While various methods may be used to simulate a lunar landing on the earth's surface by rocket- or jet-powered vehicles, these methods may not give a realistic simulation of visibility or landing site disturbance because the tests must be conducted in the earth's atmosphere. The study presented in this paper had the dual objective of investigating the feasibility of variable-cant configurations and of furnishing some correlation of future full-scale simulations in the atmosphere with what might be obtained in a near vacuum. Accordingly, tests of small-scale model variable-cant twin rockets were performed at low-ambient pressure and atmospheric-ambient-pressure conditions. Initial consideration was given to scaling the test results, but the present state of the art did not allow a practical model to full-scale ratio to be established. The tests made use of two Mach 5 nozzles to simulate rocket engines, and various combinations of sand and stone to simulate possible compositions of the lunar surface. The tests were made in the vacuum reservoir of the Langley 11-inch hypersonic tunnel.

For the discussion of the results of these studies certain rather arbitrary criteria had to be established. The tests were recorded in motion pictures which are available on loan as film supplement, NASA L-689. A request form and description of the film will be found on the page with the abstract cards.

SYMBOLS

C	single-nozzle cant angle measured with respect to vehicle X axis, deg
D	nozzle exit diameter, in.
h	nozzle height above simulated surface expressed in terms of nozzle exit diameters
p_c	nozzle chamber pressure, lb/sq in.
p_t	stagnation pressure, lb/sq in.
p_∞	ambient pressure, lb/sq in. or mm Hg

t_o starting time, sec

X longitudinal axis of vehicle

δ exhaust gas expansion angle, deg

TEST APPARATUS

Two identical Mach 5 nozzles were used to simulate the rocket engines of a space vehicle. The nozzles were convergent-divergent and had an exhaust-area-to-throat-area ratio of 25:1. A section view of the nozzle design and pertinent dimensions are shown in figure 1. The exhaust expansion characteristic of the type of nozzle used for these tests is shown in figure 2. Bottled nitrogen, oil pump grade, was used as a source of drive power for the nozzles. Nozzle chamber pressures used were 400 psi and 2000 psi; the higher pressure was used unless otherwise noted. An electrically operated valve allowed the nozzle drive to be started and stopped at will. Figure 3 shows the angles and axis system pertinent to the present investigation.

The two nozzle arrangements tested are shown in figures 4 and 5. Figure 4 illustrates the tandem arrangement, and figure 5 illustrates the crossed arrangement. Figure 6 is a pictorial view of the apparatus in test position. Relative location of the control valve, nozzles, test surface, and camera ports is shown in figure 6. The nozzle height h for this figure was 40 nozzle-exit diameters. The test chamber was 100 feet (1,920 diam) long by 8 feet (153.6 diam) in diameter. A schematic of the complete test apparatus is shown in figure 7.

Sand (U.S. Sieve Series No. 60) was used to form a bed of loose material to simulate an unprepared landing surface. Thirty tests were made with a simulated landing surface composed of sand. Seven tests incorporated a wooden link mat covered with sand. A mixture of sand and stones was used as a surface for five tests. A single test was made with a large cinderblock imbedded in each predicted blast area in a sand and stone surface. The average composition of the sand and stone surface is given in table I. The metal bed plate to hold the landing surface material was 7 feet wide (134.4 diam) by 15 feet long (288.0 diam).

Test data were obtained by photographic records and visual observation. For recording photographic records, a 16-mm movie camera operating at 128 frames per second, and a 70-mm sequence camera operating at 15 frames per second were used. A pressure-sensitive cell and a recorder were used to furnish a time history of the change in ambient pressure of the test chamber during the low ambient-pressure tests.

TESTS

The tests to determine the effect of canted rockets covered angles of from 0° to 60° in 15° increments for the crossed-nozzle arrangement. Two nozzle

heights h, 8 nozzle diameters and 40 nozzle diameters, were tested at ambient pressures p_∞ of 2 mm Hg and 1 atmosphere. The 15° cant angle was omitted for the test of $h = 8$ and $p_\infty = 1$ atmosphere. The basic depth of the simulated (sand) surface was 1.6 nozzle diameters (1 inch). The normal running time for each test was 10 seconds.

In order to determine the effect of loose particle depth cant angles of 0° and 45° were tested with a sand-bed depth of 10.66 nozzle diameters. The nozzle height was 40 diameters. The ambient pressure was 2 mm Hg.

The effect of an irregular solid substructure covered with loose material was simulated by covering a wooden link mat with sand. The sand depth over the mat was 1.6 diameters. The mat was made of interlocking wooden strips which were 0.80 diam wide by 0.96 diam high by 4.16 diam long. The open spaces in the mat were thereby 0.80 diam wide by 0.96 diam high by 2.16 diam long. Cant angles of 0° (MS 18) and 45° were tested at a height of 40 diameters at an ambient pressure of 2 mm Hg. (MS 18 indicates scene 18 in the film supplement.)

Tests were made to observe the action of particles which had sufficient mass to cause vehicle damage. The largest stones used measured approximately 2.80 diam by 1.92 diam by 0.96 diam; individual weight was approximately 0.2 pound. Tests were conducted for cant angles of 0° (MS 19), 30° (MS 21), and 45° (MS 24) at $h = 40$ diam and $p_\infty = 2$ mm Hg. Two tests were made with $C = 60°$, $h = 8$ diam, and $p_\infty = 2$ mm Hg. The sand and stone surface was 3.2 diam deep. The average composition of the sand and stone surface is given in table I.

Large boulders in the blast area were simulated by embedding a cinderblock across the center of each of the predicted blast areas. Each cinderblock weighed approximately 25 pounds and measured 8 x 8 x 16 inches (12.8 x 12.8 x 25.6 nozzle diameters). The remaining surface was covered with 3.2 diameters of the sand and stone mixture. The conditions for this test were: $C = 45°$; $h = 40$ diam, and $p_\infty = 2$ mm Hg.

Several runs were made at reduced nozzle chamber pressure (400 psi) to simulate the effect of throttled engines. Cant angles of 0° (MS 22), 30°, and 45° were tested at $h = 40$ diam. A cant angle of 60° (MS 26) was tested at $h = 8$ diam. The latter test was allowed to run for about 25 seconds. The ambient pressure for all tests at reduced chamber pressure was 2 mm Hg.

Several tests were made with the nozzles set in a tandem configuration as shown in figure 4. Two nozzle-separation distances were used. The first separation, with the nozzles set at 0° cant, was 6.4 nozzle exit diameters. The cant angles tested for this configuration were 15°, 30°, and 45°. Sand-bed depth was 1.6 diam. The second tandem nozzle separation was 9.6 nozzle exit diameters. The cant angles tested were 60° and 75°. The ambient pressure p_∞ was 2 mm Hg and the nozzle height was 8 exit diameters for both nozzle separations.

In order to establish a basis of comparison for the conditions of the tests, one single-nozzle run was made. Test parameters for the run were $C = 0°$,

h = 8 diam, p_c = 2000, and p_∞ = 2 mm Hg. The sand surface was 1.6 diam in depth. This test may be seen in MS 1.

RESULTS AND DISCUSSION

A total of 43 test runs were made during this investigation. The comments presented herein are a summation of the visual observations and notes taken during the course of the tests and a study of the film and pressure records obtained during the tests. A typical time history of the ambient pressure as recorded is shown in figure 8. An arbitrary scale was established for the visibility ratings. A visibility rating of excellent, good, fair, poor, or obscured was assigned to each run by a team of three observers. The numerical divisions of the visibility rating scale used are given in table II. The magnitude and duration of the initial starting eruption, and the accumulation of suspended debris in the immediate vicinity of the nozzles during the process of a test were the primary factors which had an effect on the level of the visibility. A span distance of 21.6 nozzle exit diameters (13.5 inches, dimension of the nozzle mount bracket) was arbitrarily chosen as the minimum horizontal dimension in the plane of cant of a landing site suitable for a satisfactory vehicle landing.

Comparison of the blast effects in low ambient pressure with those atmospheric-pressure environments indicated that much better visibility might be expected in landing on the moon's surface than in a landing under similar circumstances in the earth's atmosphere. Experience with VTOL jet aircraft landing in loose material would then give a pessimistic view of what is to be expected if a jet of equal thrust were used to land on the moon's surface. Simulation of lunar landings with rocket vehicles on earth may possibly give a realistic visibility simulation if nozzle cant angles of about 45° are used on earth to simulate the lunar landing because the visibility away from the plane of the cant will be about equal to visibility under low atmospheric-pressure conditions. However, visibility into the direction of the cant would be poor and if the vehicle were traveling in that direction, obstacles would not be seen until possibly too late for corrective action to be taken by the pilot.

On the basis of the blast effect noted in these studies, the optimum cant angle for visibility under atmospheric conditions would permit equal or better visibility under reduced ambient-pressure conditions. At low ambient pressure, h = 8 diam, the visibility was good except for the starting eruption which lasted less than 1 second. This characteristic was generally true of all nozzle cant angles. The loose material seemed to be thrown away from the blast area but not entrained in large volumes and density. Only a very light "fog" of sand particles was present and it appeared to be distributed uniformly throughout the test chamber.

Under atmospheric conditions, and lower cant angles, loose material in large volumes and high density was entrained in the nozzle blast and completely obscured vision in a direction through the stream. With the nozzles canted 30° or more, there was good visibility just below the nozzles.

A comparison of blast effects at low ambient pressure and at atmospheric pressure can be seen in figures 9 and 10 (MS 3) (see table III) with uncanted nozzles; and the comparison with nozzles canted 30° can be seen in figures 11 (MS 6) and 12 (MS 5). Continuous blasting caused heavy debris accumulation in the vicinity of the nozzles during some tests where p_∞ = 2 mm Hg. However, when the nozzle drive was stopped, the debris immediately precipitated and the visibility became excellent. The normal time delay from the end of nozzle blasting to clear visibility was approximately 0.5 second. For the tests where p_∞ = 1 atmosphere the heavier particles precipitated immediately when the nozzle blast was shut off, but the fine dust tended to remain suspended in the air for some appreciable time. In most atmospheric tests the visibility could be rated good in about 3 seconds after nozzle blast cutoff. However, an hour or more was required for the visibility to attain the level that was realized in less than 1 second following shutoff under reduced ambient pressure.

The effect of cant for the atmospheric-pressure environment was to blow the sand outward (MS 6, 8, and 10) allowing good cross-chamber visibility when the cant angle was at least 45°. Visibility into the stream was usually obscured. At angles less than 45° the landing site was cleared before the run ended. With a 45° cant, a ridge of sand was left in the center but was less than 21.6 exit diameters (assumed to be minimum required). At 60° cant the landing site was undisturbed.

The effect of cant was less pronounced in the low atmospheric-pressure environment (MS 5, 7, and 9). At all cant angles the cross-tunnel visibility was excellent after the initial starting blast. There was a slight deterioration of visibility at a cant angle of 30°, but the visibility for this configuration was still considered to be good. The general trend of the cross-tunnel visibility observed during the tests is illustrated in figure 13. Downstream visibility for corresponding angles was usually rated one step (grade scale) worse.

The canted-nozzle tests were repeated at a height of 40 exit diameters. The cross-tunnel visibility was rated good for cant angles of 0°, 30°, 45° (MS 11, 14, and 16), and 60° for the reduced ambient-pressure tests. However, as may be seen in figure 13, the maximum visibility levels attained at h = 40 diam were judged to have reached just into the minimum observed for the h = 8 diam tests. The initial eruptions were longer in duration at h = 40 diam than had been observed at h = 8 diam.

The combination of h = 40 diam, C = 15°, and p_∞ = 2 mm Hg was potentially the worst combination of conditions tested under reduced ambient pressure during this study. A sequence of this combination is shown in figure 14 (MS 13). Acceptable visibility was not realized until approximately 2.0 seconds after the initial eruption. This is approximately four times longer than the time required for the average of the other tests under reduced ambient pressure.

Corresponding tests under 1 atm at h = 40 diam indicate that an acceptable visibility level would probably not be realized unless a cant angle of at least 30° was used. In all the h = 40 tests, the downstream visibility was rated fair at best. The cross-tunnel visibility and the downstream visibility

were approximately equal for a cant angle of 0°. The visibility, as for h = 8 diam, tended to deteriorate with time for tests with a cant angle of 60°.

For the tests at h = 40 diam the sand-bed area under the nozzles was blown clear at nozzle cant angles of 0° and 15° for both ambient-pressure conditions. At 30° the remaining sand-bed span was usually about equal to the span of the nozzle mount bracket. At 45° and at 60° the landing site was undisturbed.

For several of the tests at h = 40 diam a ball of black lint approximately 0.5 inch in diameter was placed on the sand-bed surface directly under the pivot axis of the nozzles. The intended purpose of this lint was to serve as a point of focus for the photographer. An inspection of the photographic records revealed that the lint also served as an excellent indication of the flow characteristic directly under the nozzles during the tests. At a cant angle of 45° (two tests involved at p_∞ = 2 mm Hg, two tests at p_∞ = 1 atm) the lint was visible throughout each of the tests. Its position did not shift during the run, and sand deposit in its area was sufficient only to coat the lint with a thin layer of fine sand dust. No burying effect was noted. At a cant angle of 30° (one run involved at p_∞ = 2 mm Hg) the lint was carried away by a small plume of sand which existed directly under the nozzles for a very short time during the initial starting eruption.

Blast damage to the proposed touchdown site appeared to be a function of cant angle, nozzle height, and ambient pressure. Figure 15 indicates the trend of the blast effect on the surface directly under the nozzles. This is a summation of all tests that have thus far been discussed and is not intended to illustrate the result of a single set of parameters. Under reduced ambient pressure and at the lower height, a larger cant angle than was required for p_∞ = 1 atm was necessary to insure a remaining area which had the assumed minimum span of 21.6 nozzle exit diameters.

Reference 1 poses the question as to whether the buildup of a pile of particles (as found in ref. 1) under the center of the nozzle was a starting transient effect, or a function of nozzle design. Particle buildup under the center of the nozzles for the tests covered in this paper appeared definitely to be a starting transient effect. For cant angles of 0° (MS 11) and 15° (MS 13), h = 40, p_∞ = 2 mm Hg the initial starting phenomena indicated that a buildup began to form, but as soon as the flow had become established the situation disappeared. An indication of the starting phenomena involving particle buildup may be seen in figure 14.

For all conditions tested, a cant angle of 45° appeared to be optimum. Heavier debris was usually present for cant angles less than 45°. In excess of 45° cant the starting visibility was generally good, but frequently deteriorated as the run progressed in time. Under low ambient-pressure conditions, a cant angle of 0° and a cant angle of 45° were rated approximately equal in terms of visibility.

A sand depth of 10.88 diameters (MS 20) was used to investigate the effect of a relatively deep (compared with other tests in this study) loose material

surface. For the first cant angle, $C = 0^{\circ}$ (p_{∞} = 2 mm Hg; h = 40 diam) the initial eruption was about average in volume but comparatively long in duration. After the initial crater had been dug, periodic bursts of sand would erupt from the crater. It appeared that the crater wall surfaces were collapsing, sliding to the bottom of the crater, then being blown upward by the nozzle blast. The resultant crater measured 44.8 diameters across the top and 9.6 diameters across the bottom. The metal bed plate was exposed. At a cant angle of 45° there did not appear to be any particular difference in visibility or surface disturbance from that observed in the $C = 45^{\circ}$ tests with a sand depth of 1.6 diameters.

The tests with an irregular solid substructure, an interlocking wooden mat (MS 18), were conducted to determine if, after the initial layer of surface sand had been blown away, the pockets of sand contained by the mat would tend to erupt individually. No individual "pocket" eruptions were observed. The initial eruptions, volume of debris in vicinity, visibility, etc., did not appear to be any different from the other tests performed with 1 inch of sand on a smooth metal board. The downstream sand crater walls were usually "streaked" by the deflected flow from the mat "pockets."

Tests were made to observe the action of particles which had sufficient mass to cause vehicle damage. The action observed during the blasting of the sand and stone surface did not appear to differ materially from the tests with a surface made up of sand only. At no time during these tests were particles, sand or stones, observed to strike the nozzles. Visual inspection of the nozzles and support bracket did not disclose any evidence of damage caused by debris. Debris was observed to strike the nozzles repeatedly during the tests discussed in reference 1.

Large boulders in the blast area were simulated by placing a cinderblock across the center of each of the predicted blast areas. A comparison of three test runs was made to determine the effect of the cinderblock being in the blast area. The test conditions for each of the three runs compared were as follows:

Run	Cant angle, C, deg	Nozzle height, h, diam	Ambient pressure, p_{∞}, mm Hg	Surface	
				Material	Height, diam
1	30	40	2	Sand and stone	3.2
2	45	40	2	Sand and stone	3.2
3	45	40	2	Sand and stone plus cinder-block across surface blast area	3.2

The volume of debris blasted up and flying in the immediate area of the nozzles during run 1, $C = 30^{\circ}$, was approximately twice that observed during run 2, $C = 45^{\circ}$. The presence of the cinderblock which acted as a retaining wall (run 3; $C = 45^{\circ}$), caused the volume of debris in the vicinity of the nozzles to equal or exceed the volume of debris observed during run 1 for a cant angle of 30°. The cinderblock position did not shift during the test run.

Reduced nozzle chamber pressure was used to test the effect of engine throttling ($h = 40$; $p_{\infty} = 2$ mm Hg). The initial starting eruptions were very mild and of short duration. At $C = 0^{\circ}$ (MS 22), the cross-tunnel and downstream visibility were rated fair to good. For cant angles of 30° (MS 23) and 45°, the cross-tunnel visibility varied from good to excellent and downstream visibility varied from fair to good. At $C = 0^{\circ}$, the landing site was destroyed. At $C = 30^{\circ}$ and 45°, the landing site was undisturbed.

One reduced chamber-pressure test was made at $C = 60^{\circ}$, $h = 8$, and $p_{\infty} = 2$ mm Hg (MS 26). The nozzles were allowed to blast for approximately 25 seconds. The initial eruption was small and of short duration. Cross-tunnel visibility at the beginning of the blast was excellent. This gradually deteriorated during the tests until at the end, the visibility was poor. Downstream visibility deteriorated from good to very poor. The landing-site area remaining undisturbed at the end of the test was less than the minimum assumed required.

Several test runs were made with the nozzles set in a tandem configuration as shown in figure 4. For the smaller separation, the cross-tunnel visibility ranged from good to excellent. Downstream visibility was generally fair to good. At $C = 45^{\circ}$, $p_{\infty} = 1$ atmosphere (for $p_{\infty} = 2$ mm Hg, downstream visibility for $C = 45^{\circ}$ was good) the downstream visibility was rated as poor. At a cant angle of 15° the sand-bed disturbance under the nozzle was considered sufficient to have damaged the surface to an extent that a satisfactory landing area did not remain. For the $C = 30^{\circ}$ and $C = 45^{\circ}$ test runs, the sand-bed disturbance under the nozzles was small enough to consider the prospective landing site undisturbed.

At the larger tandem nozzle separation, the visibility during each of the tests was considered good to excellent, and the landing site was undisturbed at the end of each test.

In general, the visibility and the landing-site disturbance for the tandem configuration were rated slightly better than for the same factors for the nozzles in the crossed configuration. However, the nozzle separation for the crossed configuration was considered more representative of a practical vehicle-diameter-to-nozzle-exit-diameter ratio.

Comparison of the blast effects of a single nozzle with the blast effects of a twin-nozzle configuration can be made from the photographs in figures 9 and 16. The nozzles for the twin-nozzle configuration were spaced 2.72 exit diameter between centers. Both the single- and twin-nozzle configurations were at zero cant angle. The blast effects of the two configurations in the low-pressure environment were essentially the same. The one notable exception was

the brief formation of a four-leaf clover pattern apparently resulting from a flow interference of the twin nozzles. Initially, the starting blast of the single nozzle cleared an area approximately 17.6 nozzle diam in diameter. The cleared area was surrounded by a rim of sand which was higher than the initial sand-bed surface. As the run progressed, sand was blown from the rim outward at approximately the same rate as sand was blown from just outside the rim. As a result, a ring of sand persisted for some time after the center and outside areas had been blown clear. The remaining sand ring was about 2 inches wide. Some inflow of sand was evident by the reduction of diameter of the cleared area between the time of the initial eruption and the formation of the sand ring. After about 10 seconds of operation, a large area below the nozzle was completely cleared. The visibility was excellent except for the initial starting blast. A low-density, uniform, "haze" of sand particles persisted after the starting blast.

The results of the single-nozzle test indicate that, although the flow from the nozzle must expand in the low atmospheric-pressure environment, the high-velocity "core" of the flow has the greatest blast effect on the loose sand below the nozzle. This conclusion is consistent with the pressure measurements shown in figure 17. These measurements were obtained by Allen R. Vick and Earl H. Andrews, Jr., in the 41-foot-diameter vacuum sphere at the Langley Research Center.

CONCLUDING REMARKS

Two Mach 5 nozzles were used to simulate the rocket engines of a space vehicle which would be capable of making a vertical lunar descent and landing. On the basis of the blast effects noted in these tests, the optimum cant angle for visibility under atmospheric conditions would permit equal or better visibility under reduced ambient-pressure conditions. For all conditions tested, a cant angle of 45° appeared to be optimum. Heavy debris was usually present in the vicinity of the nozzles for cant angles less than 45°. For cant angles, in excess of 45°, the starting visibility was generally good, but frequently deteriorated as the run progressed in time. Under low ambient-pressure conditions a cant angle of 0° and a cant angle of 45° were rated approximately equal in terms of visibility.

The tests indicate that in a lunar landing, rapid clearing of the touchdown area will occur as a vehicle descends vertically to the surface with an uncanted rocket engine or engines. To be comparable with the tests, however, the landing surface would be a solid rock underlayer covered by loose material. Excess depths of loose material could preclude a successful landing of a vehicle using uncanted nozzles.

At no time during these tests was debris observed to strike the nozzles. Visual inspection, following each of the tests, of the nozzles and support bracket did not disclose any evidence of damage caused by debris.

Langley Research Center,
National Aeronautics and Space Administration,
Langley Station, Hampton, Va., August 13, 1964.

REFERENCES

1. Spady, Amos A., Jr.: An Exploratory Investigation of Jet-Blast Effects on a Dust-Covered Surface at Low Ambient Pressure. NASA TN D-1017, 1962.

2. Grossman, Robert L.: Characteristics of Particles Blown Away by Exhaust Jet Impingement on a Lunar Surface. Rept. No. ADR 04-04-62.3, Grumman Aircraft Eng. Corp., Dec. 1962.

3. Roberts, Leonard: The Action of a Hypersonic Jet on a Dust Layer. Paper No. 63-50, Inst. Aerospace Sci., Jan. 1963.

4. Sibulkin, M.; and Gallaher, W. H.: Some Aspects of the Interaction of a Jet With a Dust Covered Surface in a Vacuum Environment. Rept. ERR-AN-9403 (Contract No. REA 111-9403), Eng. Dept. Gen. Dyn/Astronaut., Feb. 10, 1963.

5. Stitt, Leonard E.: Interaction of Highly Underexpanded Jets With Simulated Lunar Surfaces. NASA TN D-1095, 1961.

6. Bauer, R. C.; and Schlumpf, R. L.: Experimental Investigation of Free Jet Impingement on a Flat Plate. AEDC-TN-60-223 (Contract No. AF 40(600)-800 S/A 11(60-110)), Arnold Eng. Dev. Center, Mar. 1961.

TABLE I.- COMPOSITION OF SAND AND STONE MIXTURE

[Larger individual particles 2.80 by 1.92 by 1.96 diams; size = 1.75 by 1.2 by 0.6 in.; weight = 0.2 lb]

Particle size, in.	Nozzle diameters	Percent by weight	Percent by volume
≧ 1/2	0.80	33.2	21
≧ 1/4	.40	10.6	3
≧ 1/8	.20	5	.9
≧ 1/16	.10	1.7	.1
< 1/16	.10	49	75

TABLE II.- VISIBILITY RATING SCALE

Word rating	Numerical rating	Verbal description
Excellent	10 - 9	All test components (as viewed by an observer through a camera port) clearly visible. Volume of airborne sand debris in vicinity of nozzles negligible. Conscious effort required for observer to realize flying debris across system.
Good	8 - 7	All test components visible. Debris evident.
Fair	6 - 5	Test components hazy but outline plainly evident.
Poor	4 - 3	Outline of test components blurred. Observer not definitely able to distinguish reference objects.
Obscured	2 - 1	Outline of test components partly obscured or invisible. Volume of debris excessive.

TABLE III.- AVAILABLE 16-MM FILM SUPPLEMENT

[NASA Film Serial No. L-689, Black and White, Silent]

Movie scene	Cant angle, deg	p_∞	p_c, psi	Surface material depth, in.	Height, exit diameters
Reel I Running time: 15 minutes at 24 frames/second					
1	[a]0	2 mm Hg	2000	1 inch sand	8
2	0	2 mm Hg	2000	1 inch sand	8
3	0	1 atm	2000	1 inch sand	8
4	15	2 mm Hg	2000	1 inch sand	8
5	30	2 mm Hg	2000	1 inch sand	8
6	30	1 atm	2000	1 inch sand	8
7	45	2 mm Hg	2000	1 inch sand	8
8	45	1 atm	2000	1 inch sand	8
9	60	2 mm Hg	2000	1 inch sand	8
10	60	1 atm	2000	1 inch sand	8
Reel II Running time: 25 minutes at 24 frames/sec					
11	0	2 mm Hg	2000	1 inch sand	40
12	0	1 atm	2000	1 inch sand	40
13	15	2 mm Hg	2000	1 inch sand	40
14	30	2 mm Hg	2000	1 inch sand	40
15	30	1 atm	2000	1 inch sand	40
16	45	2 mm Hg	2000	1 inch sand	40
17	45	1 atm	2000	1 inch sand	40
18	0	2 mm Hg	2000	1 inch sand on wooden mat	40
19	0	2 mm Hg	2000	2 inches of sand and stones	40
20	0	2 mm Hg	2000	6 inches sand	40
21	30	2 mm Hg	2000	2 inches sand and stones	40
22	0	2 mm Hg	400	1 inch sand on mat	40
23	30	2 mm Hg	400	1 inch sand	40
24	45	2 mm Hg	2000	2 inches sand	40
25	60	2 mm Hg	2000	2 inches sand and stones	8
26	60	2 mm Hg	400	2 inches sand and stones	8

[a]Single nozzle.

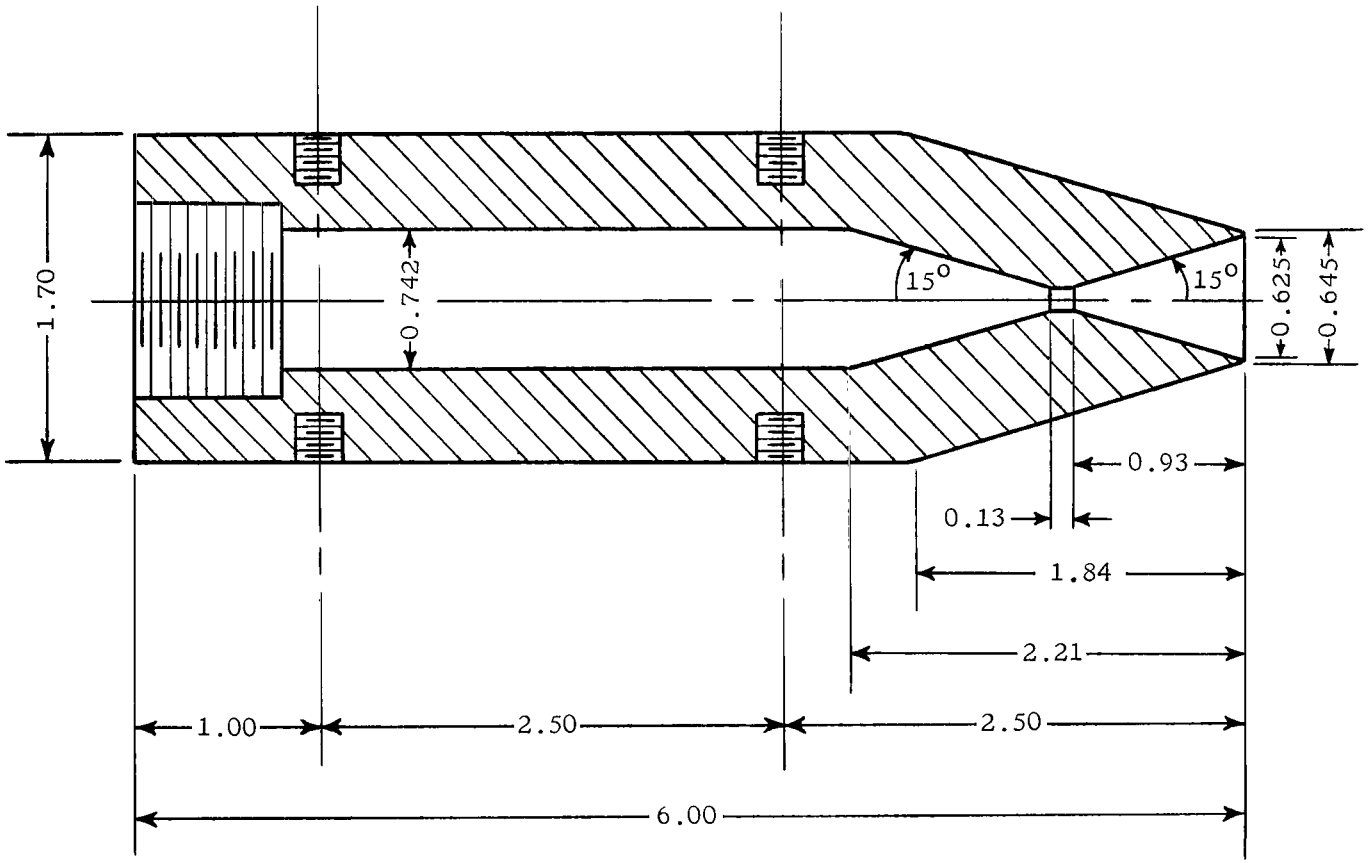

Figure 1.- Section drawing of test nozzle. All dimensions are in inches.

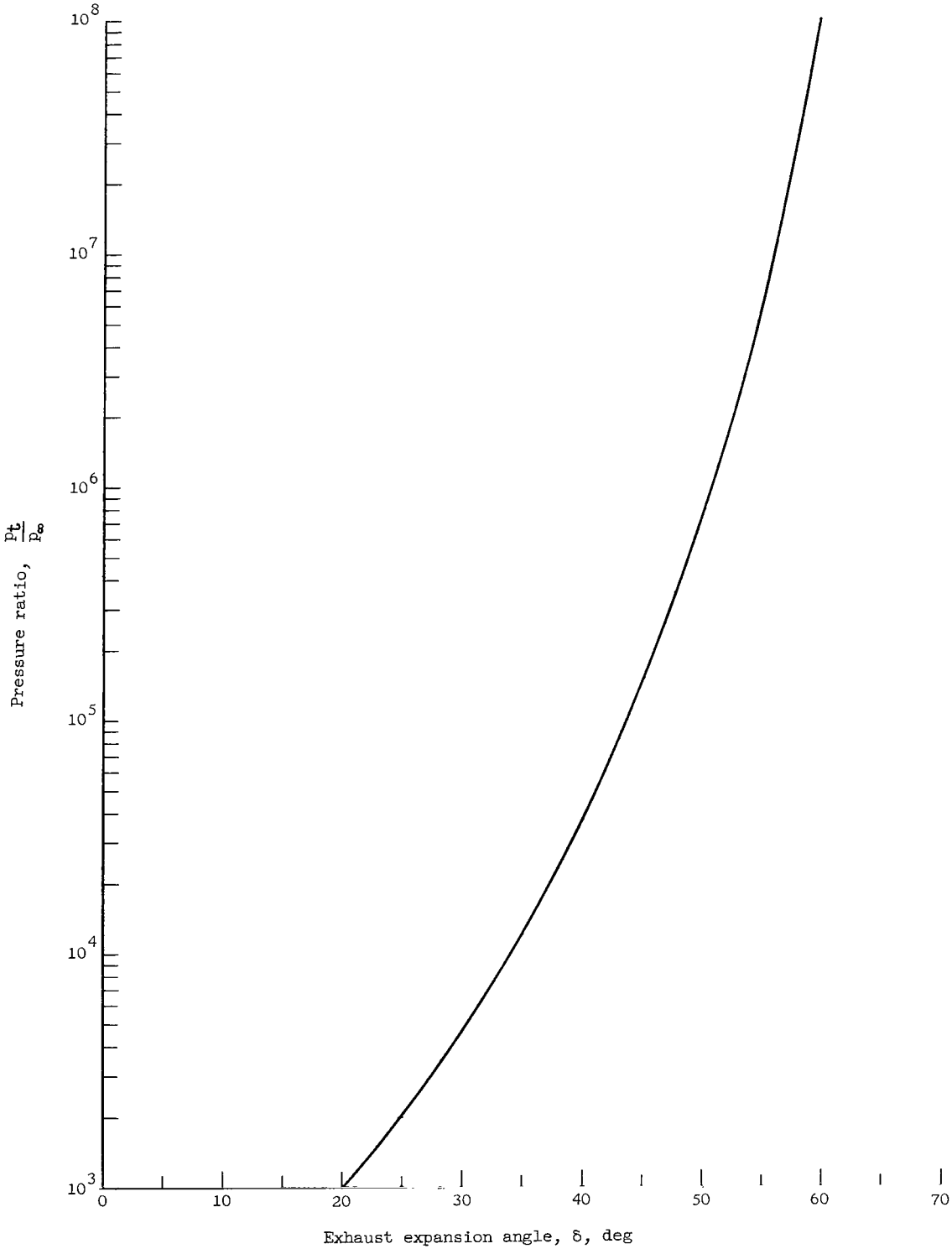

Figure 2.- Exhaust-expansion characteristic of the nozzle type used for present tests.

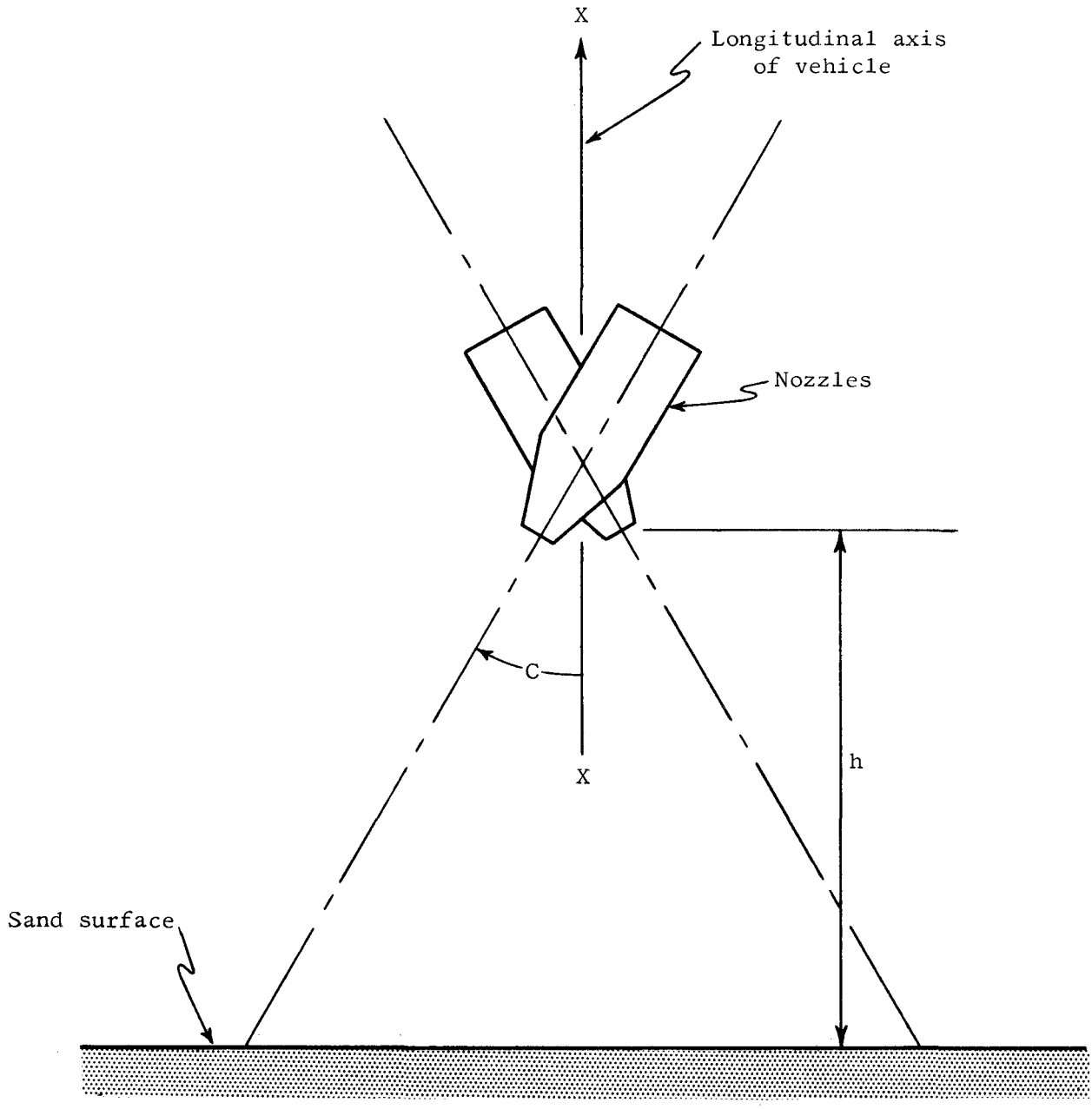

Figure 3.- Axis system.

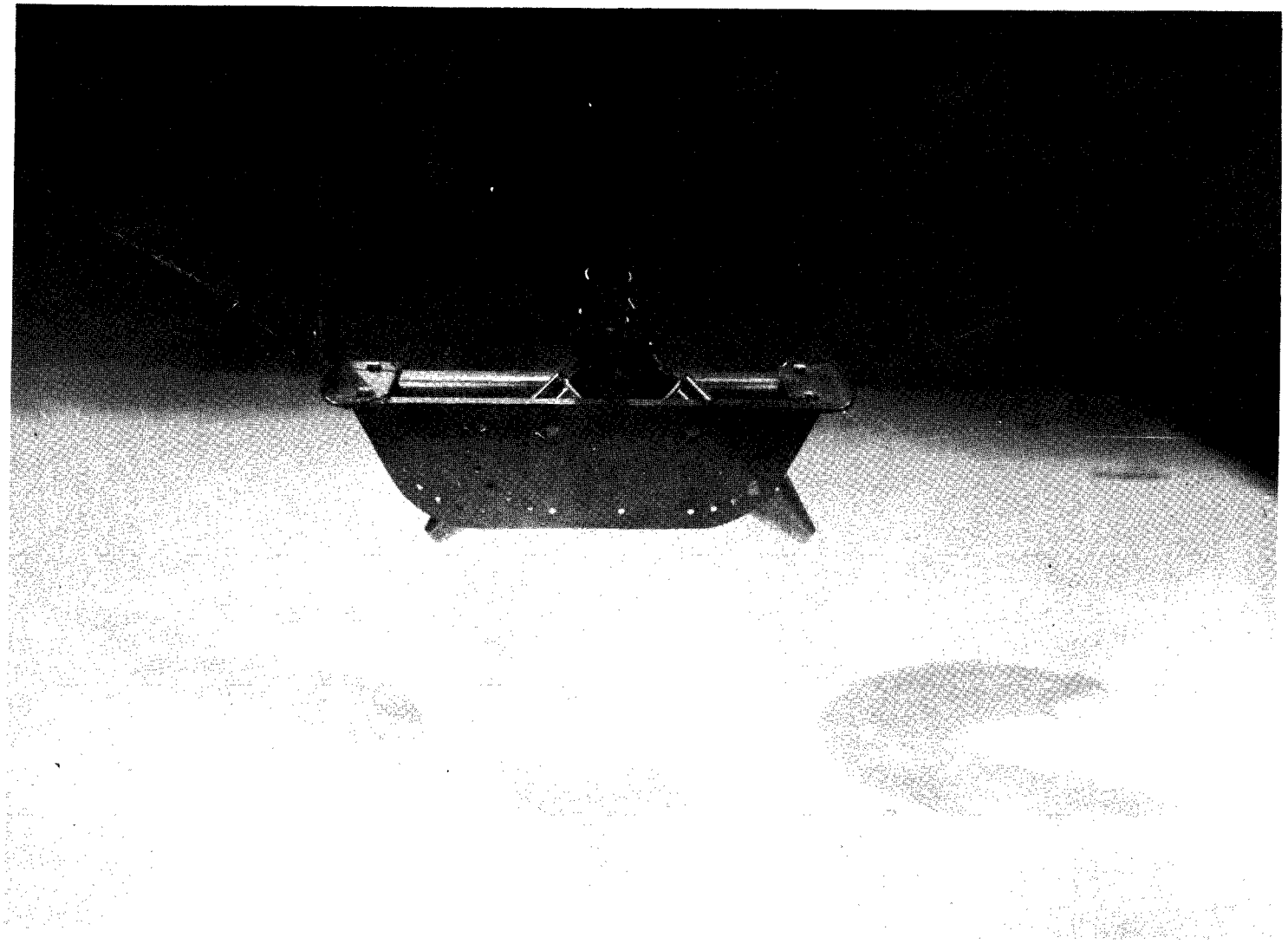

Figure 4.- Tandem-nozzle arrangement.

L-62-645

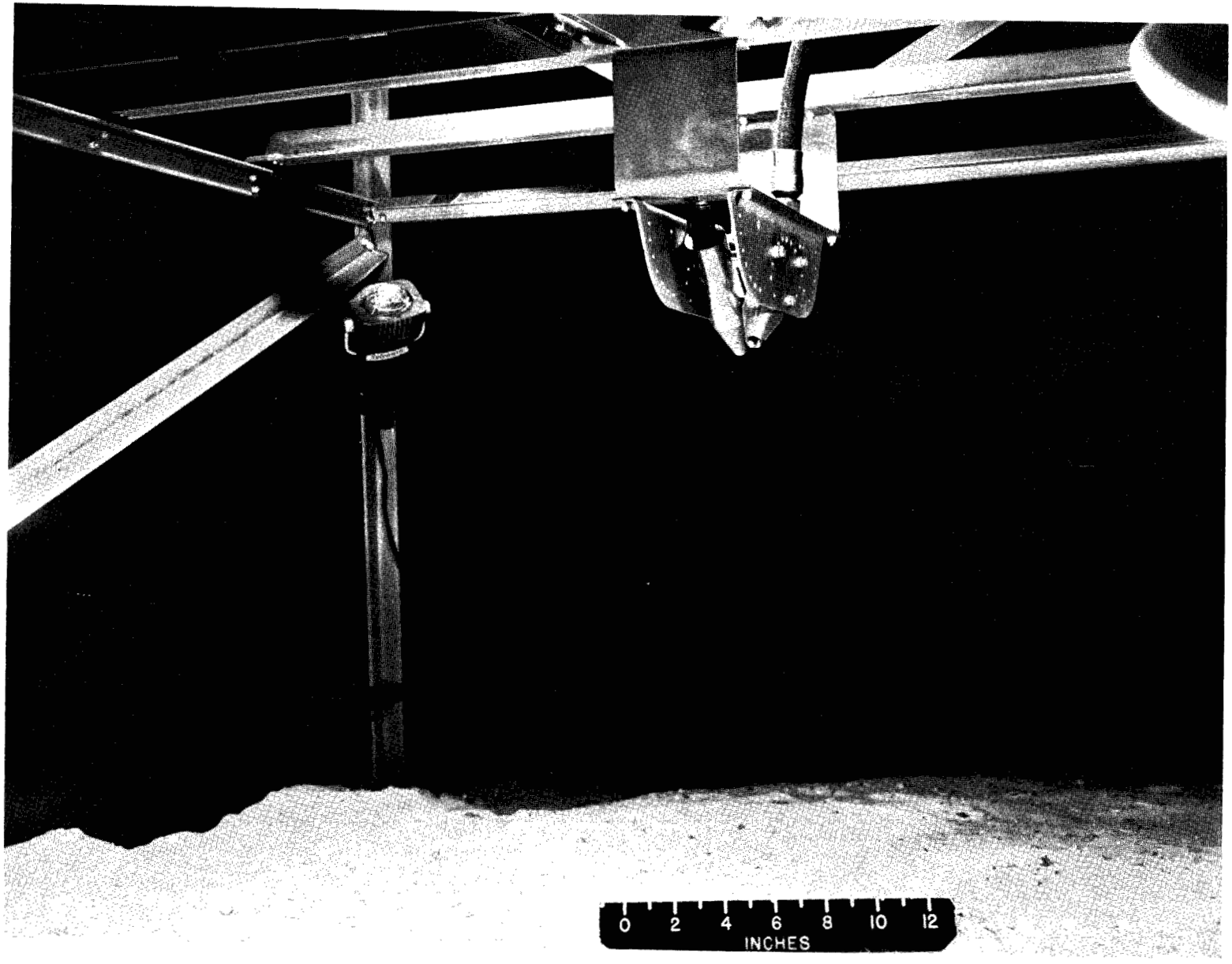

Figure 5.- Crossed-nozzle arrangement.

L-62-1550

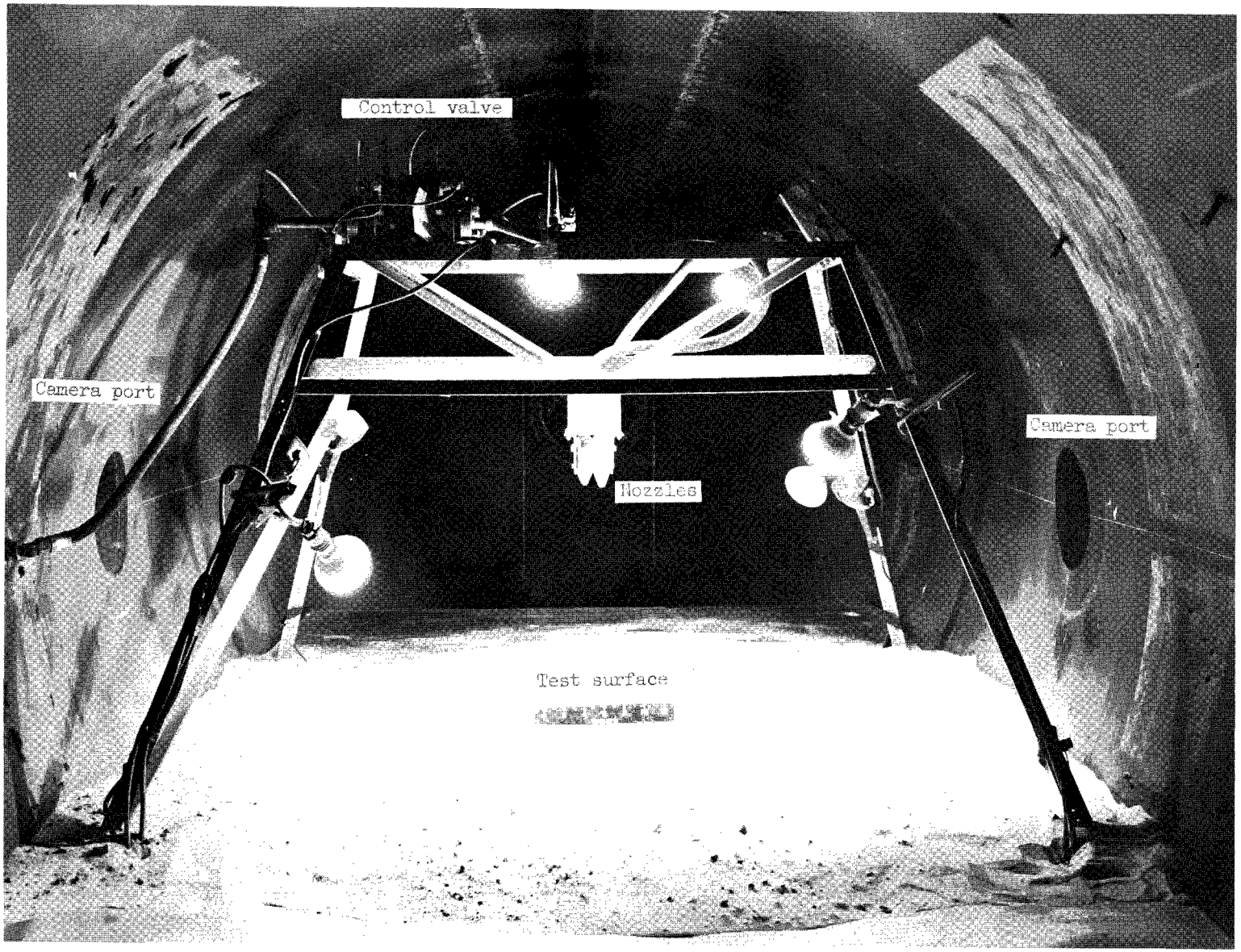

Figure 6.- Overall view of test apparatus. L-62-1549.1

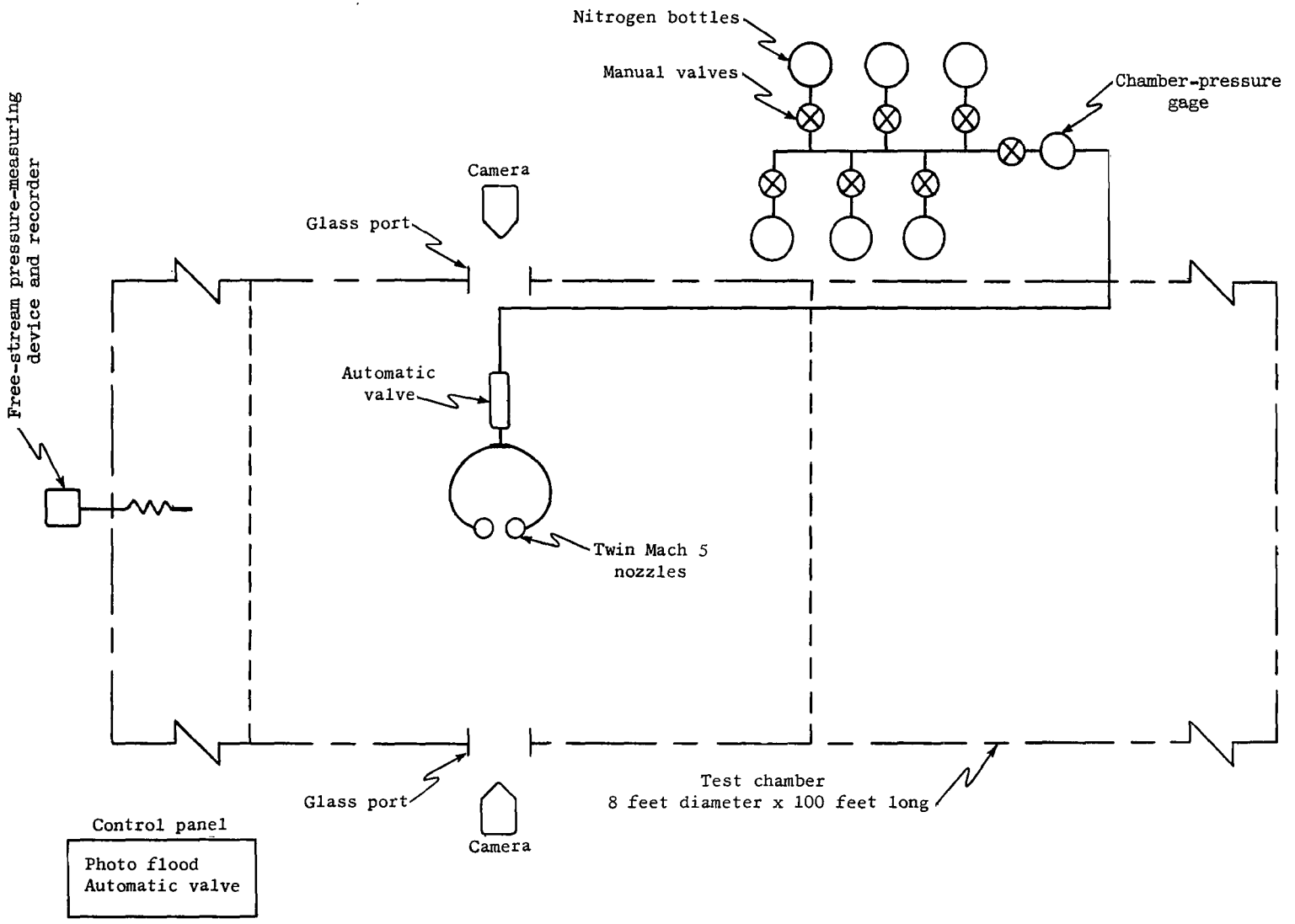

Figure 7.- Schematic of test apparatus.

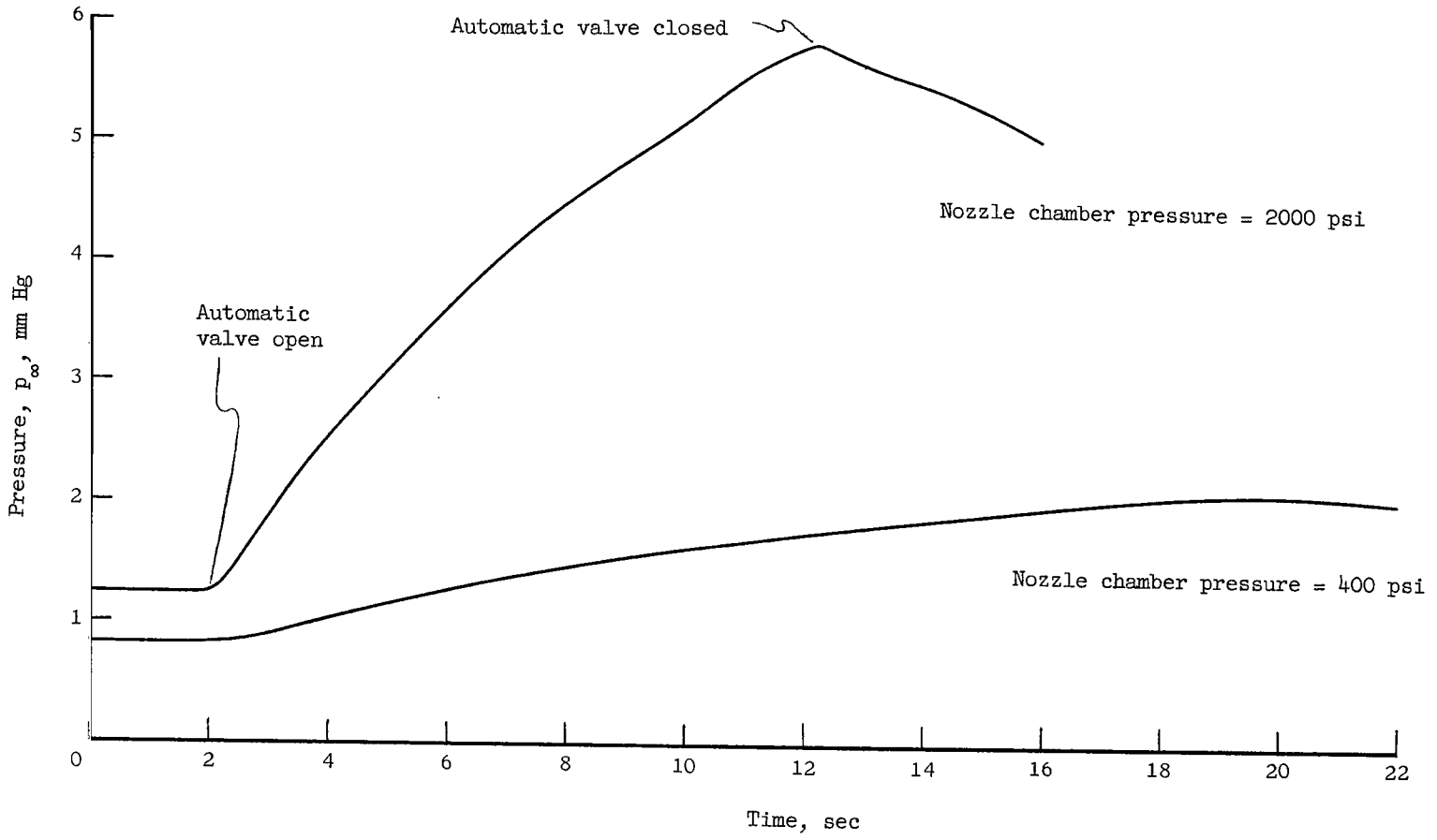

Figure 8.- Typical change in ambient pressure during tests made under low-ambient-pressure conditions.

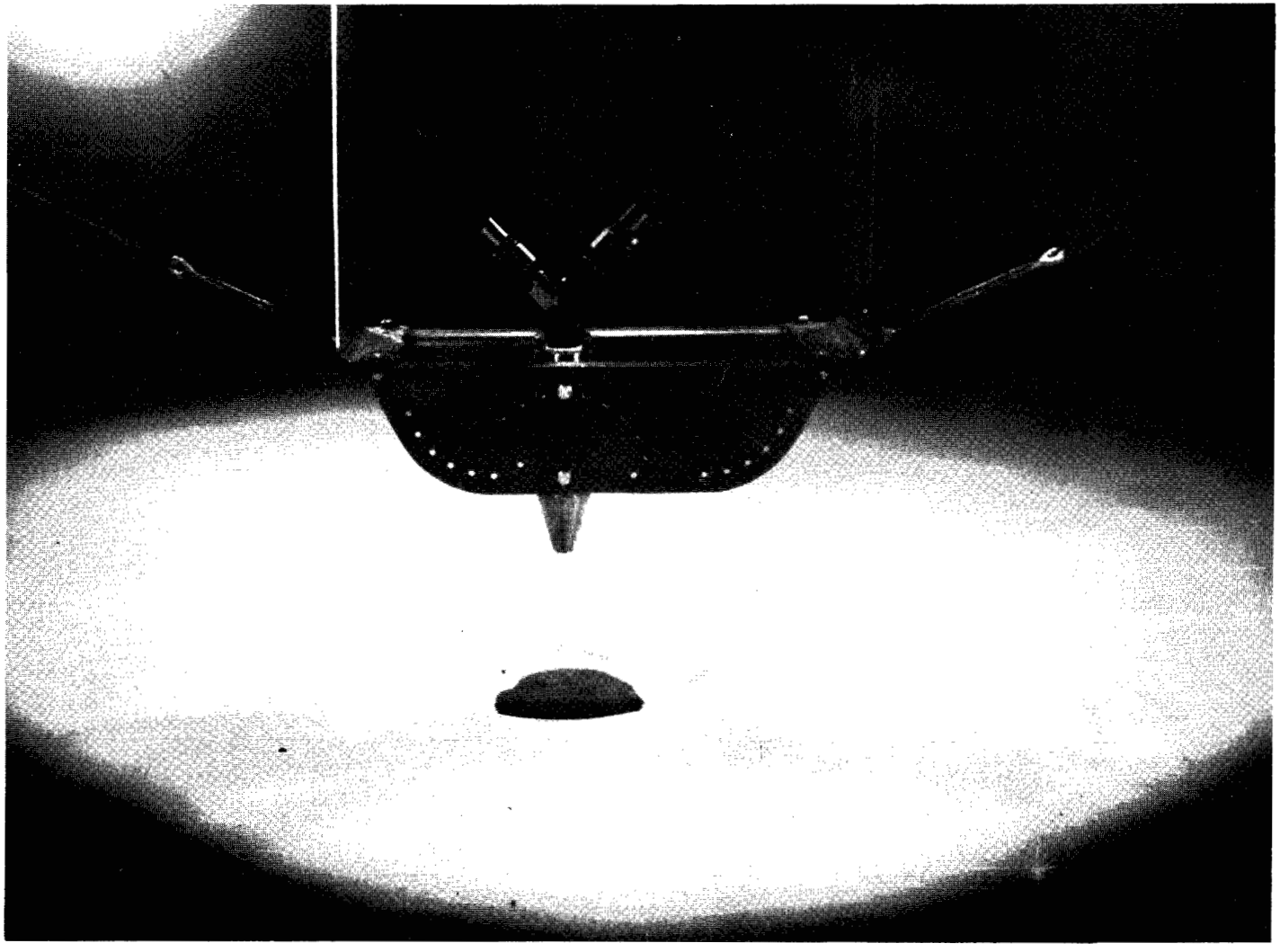

(a) Static conditions. L-64-4755

Figure 9.- A photographic sequence of the twin nozzles. p_∞ = 2 mm Hg; C = 0°; h = 8 nozzle exit diameters; p_c = 2000 psi; sand-bed depth = 1.6 nozzle diam.

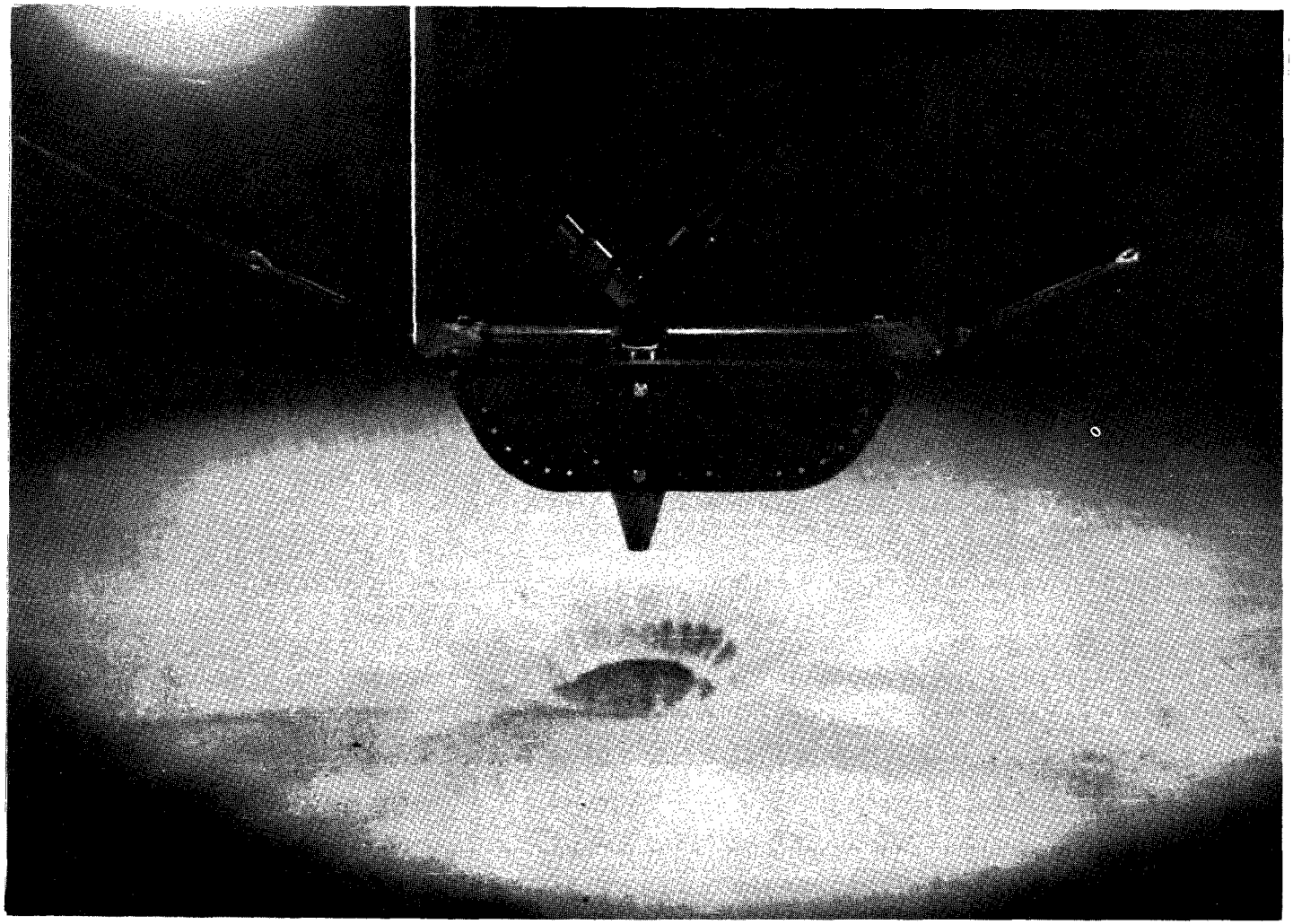

(b) Initial blast, t_o.

L-64-4756

Figure 9.- Continued.

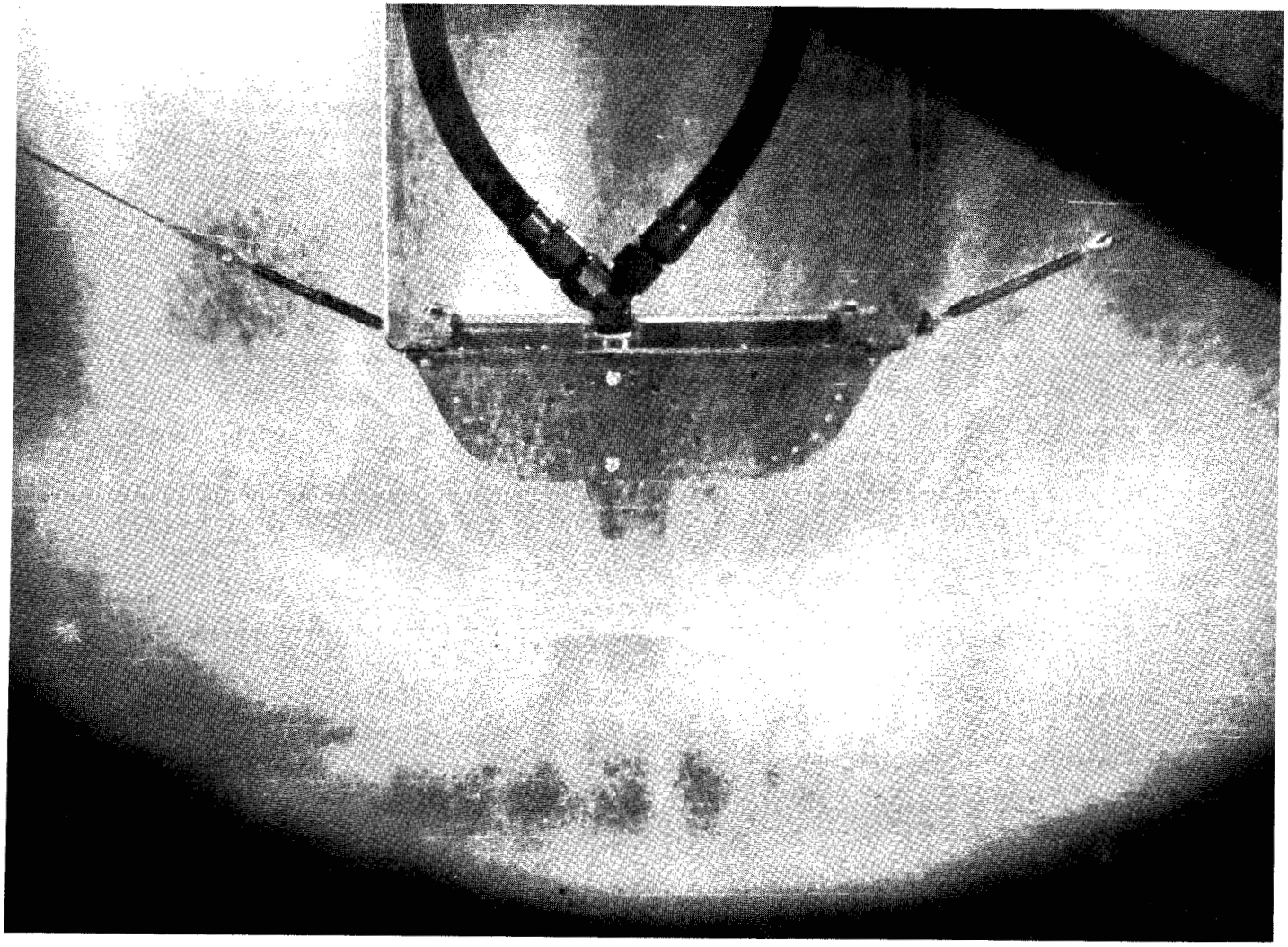

(c) t_o + 0.133 second. L-64-4757

Figure 9.- Continued.

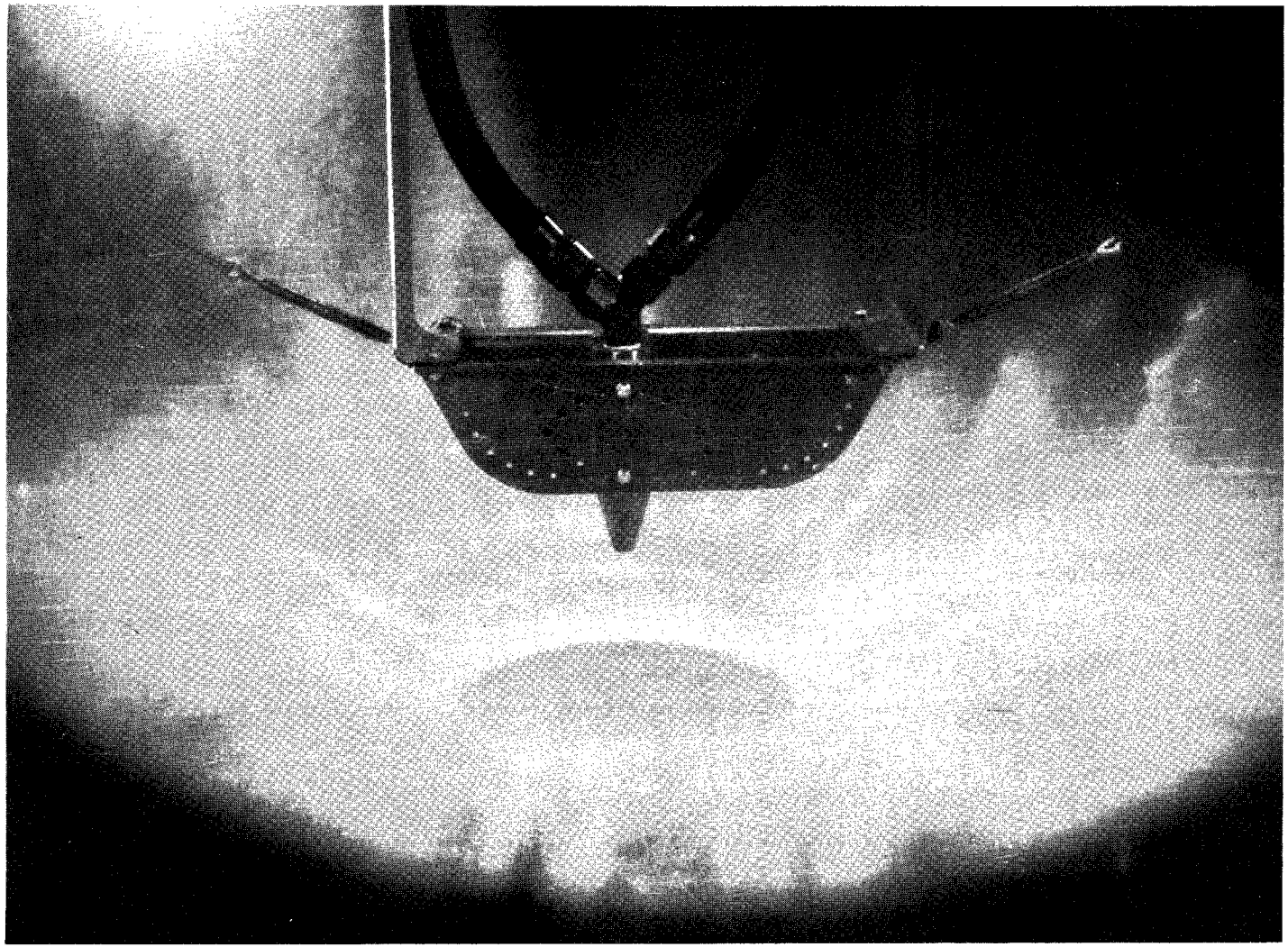

(d) t_o + 0.200 second. L-64-4758

Figure 9.- Continued.

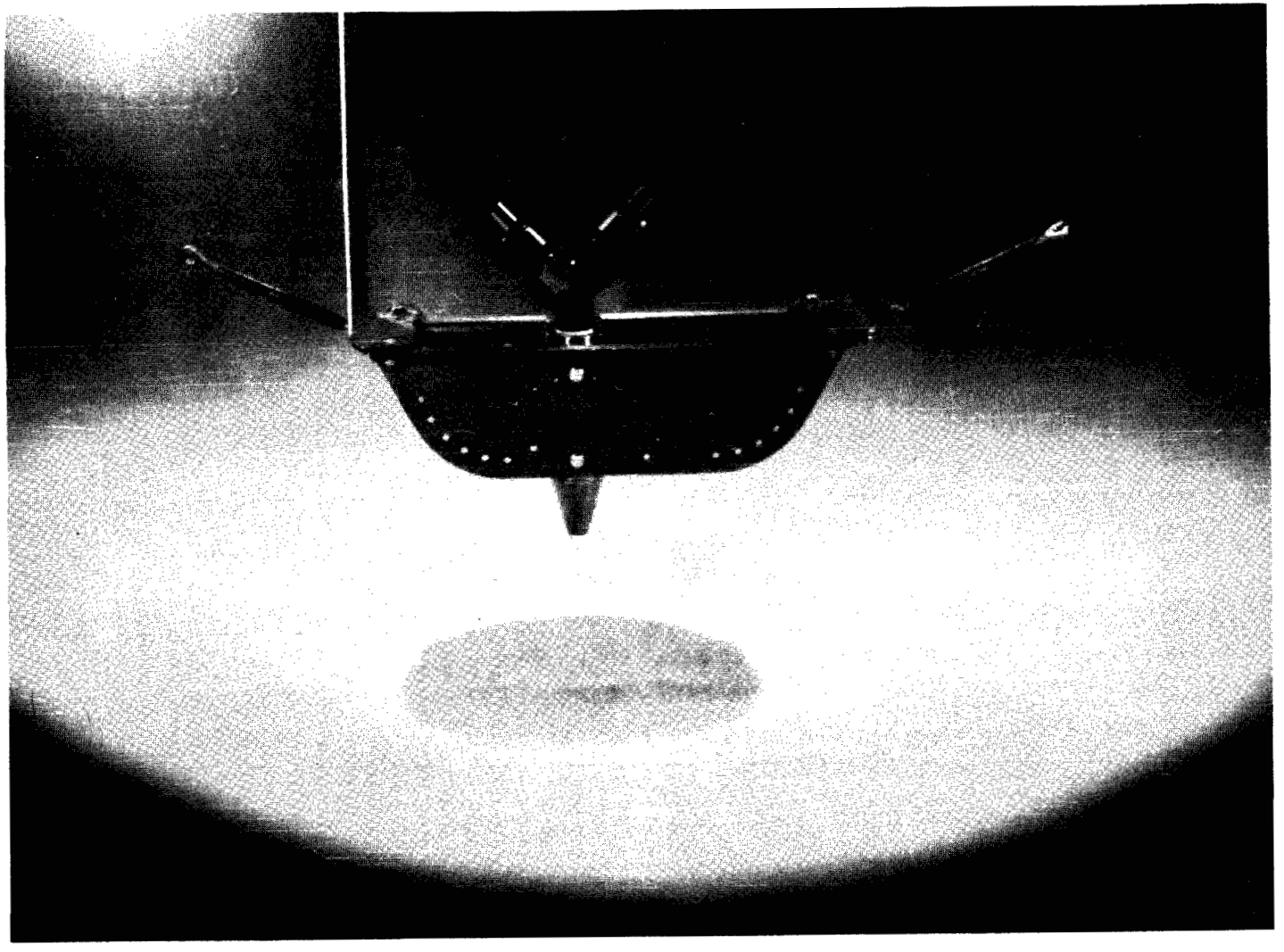

(e) t_o + 0.333 second. L-64-4759

Figure 9.- Continued.

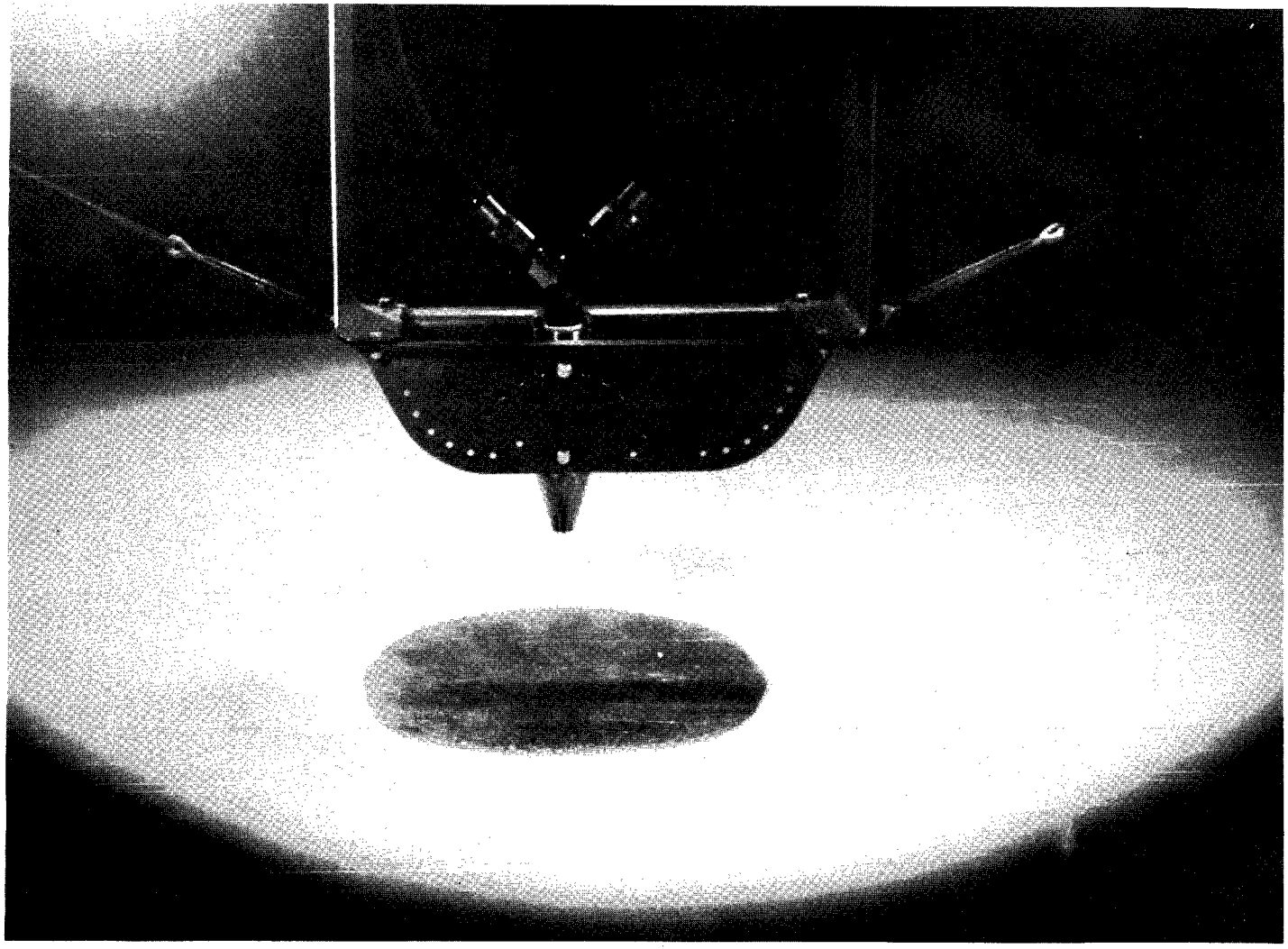

(f) t_o + 1.000 second. L-64-4760

Figure 9.- Continued.

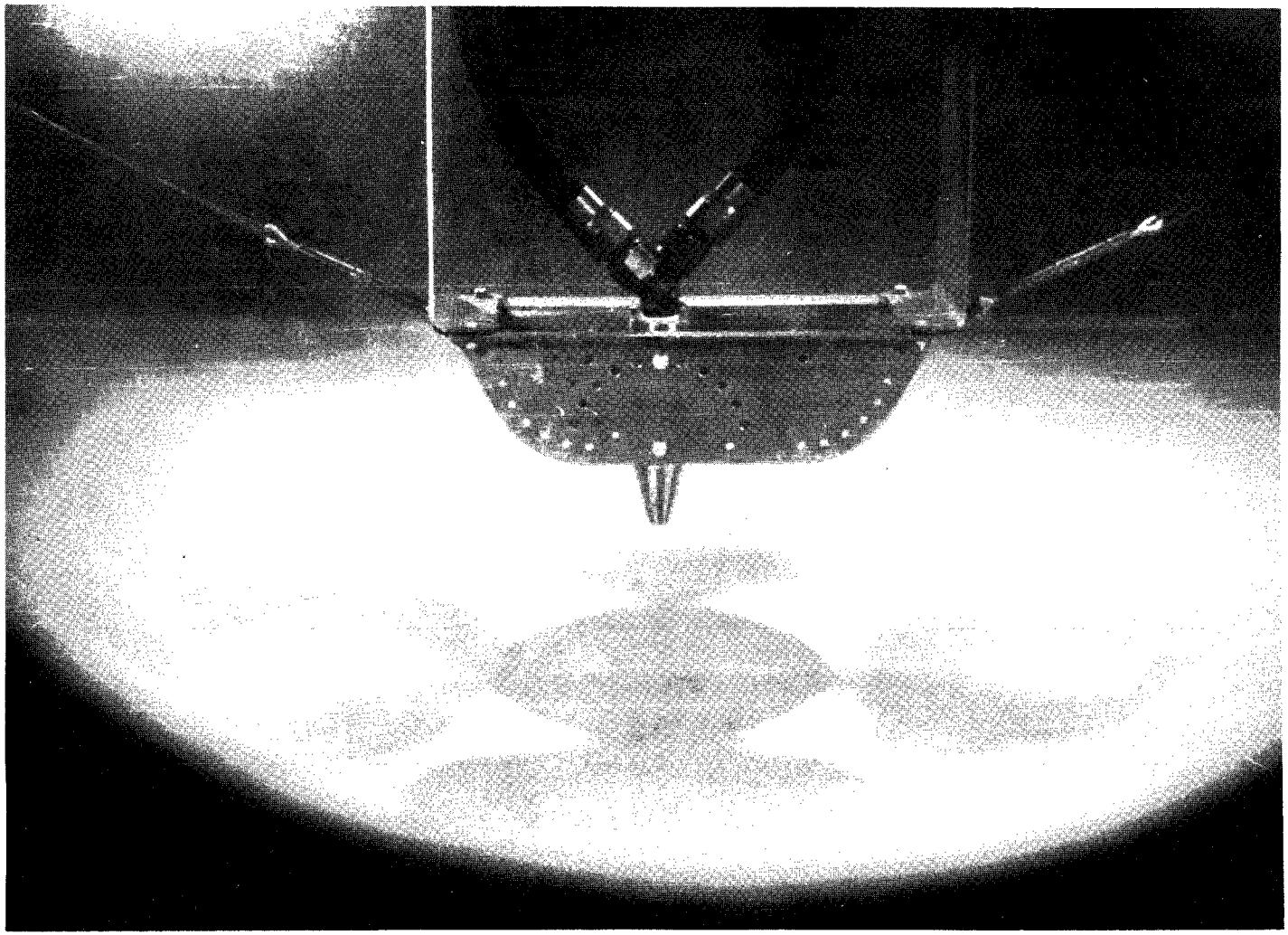

(g) t_o + 8.067 seconds. L-64-4761

Figure 9.- Continued.

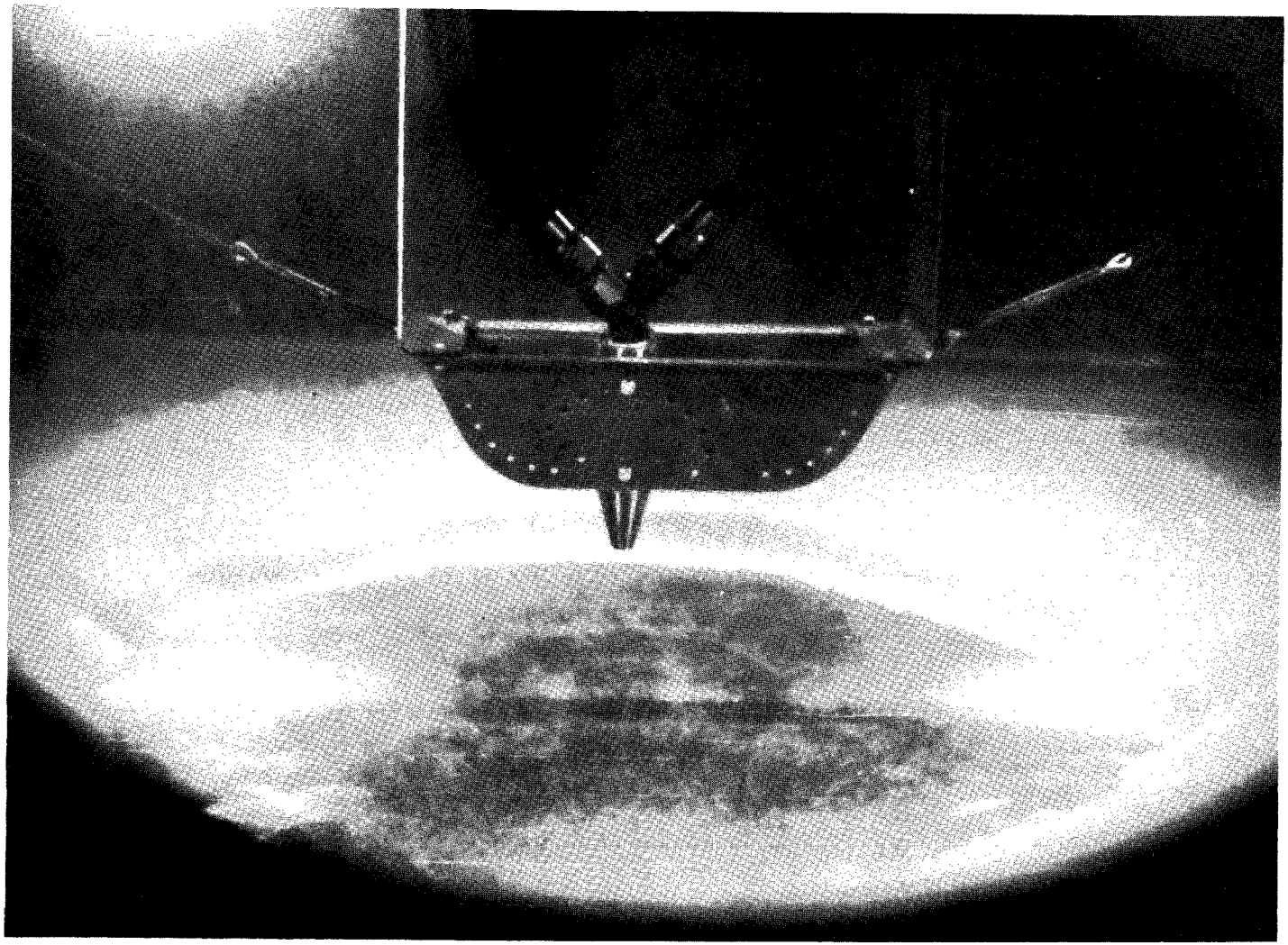

(h) t_o + 10.000 seconds. L-64-4762

Figure 9.- Concluded.

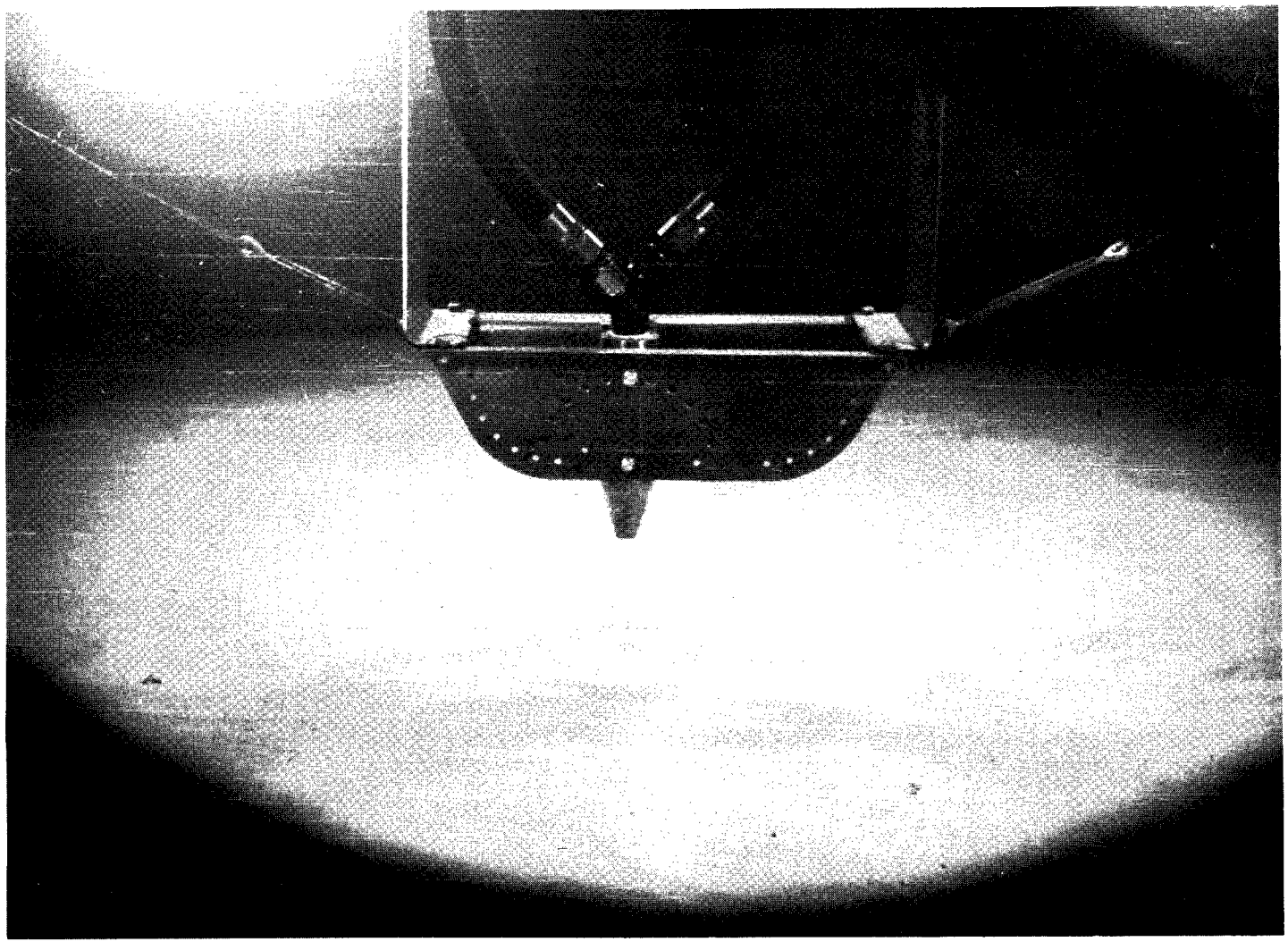

(a) Static conditions. L-64-4763

Figure 10.- Photographic sequence of the twin nozzles. p_∞ = 1 atm; C = 0°; h = 8 nozzle exit diameters; p_c = 2000 psi; sand-bed depth = 1.6 nozzle diam.

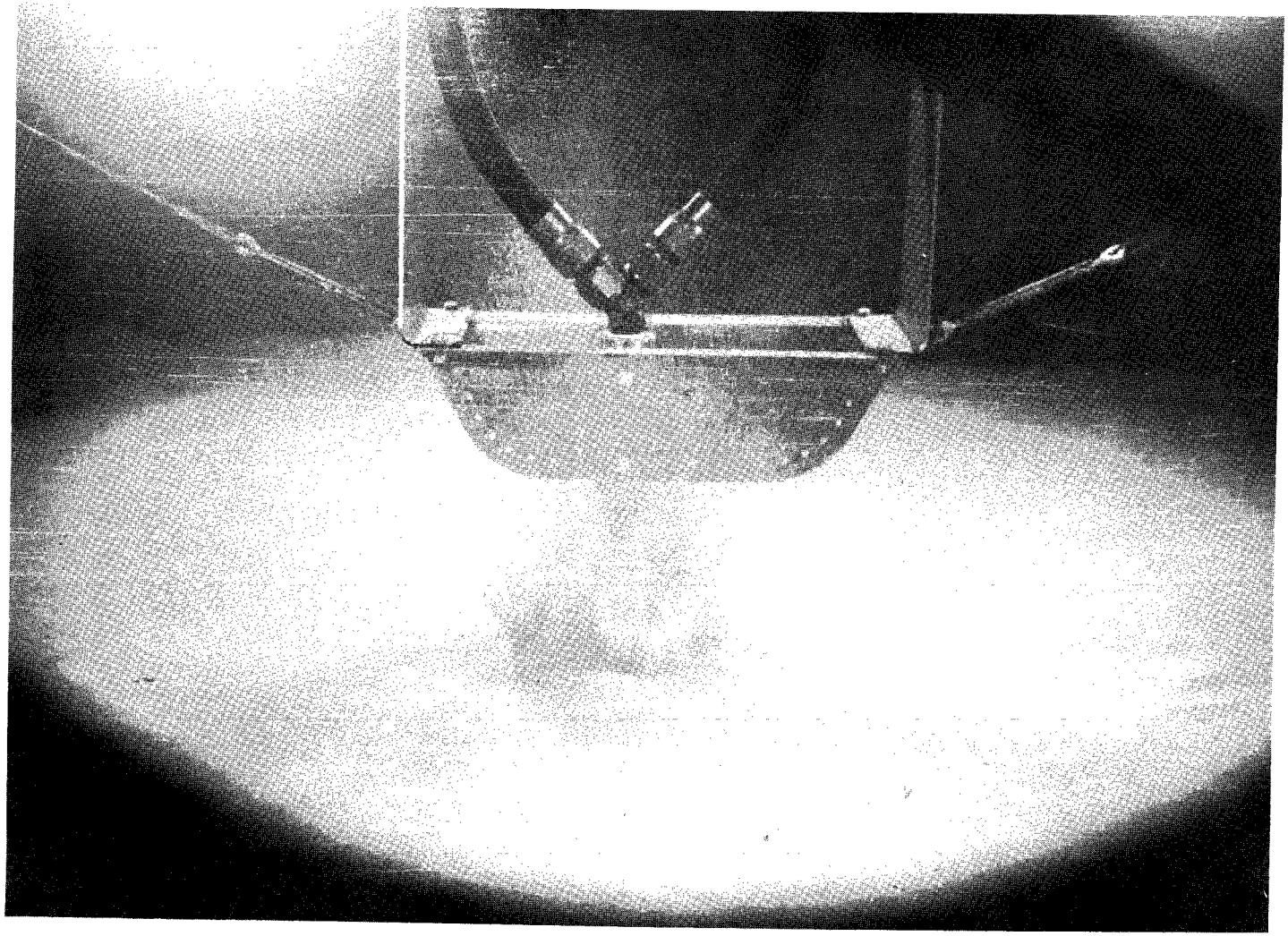

(b) Initial blast, t_o.

L-64-4764

Figure 10.- Continued.

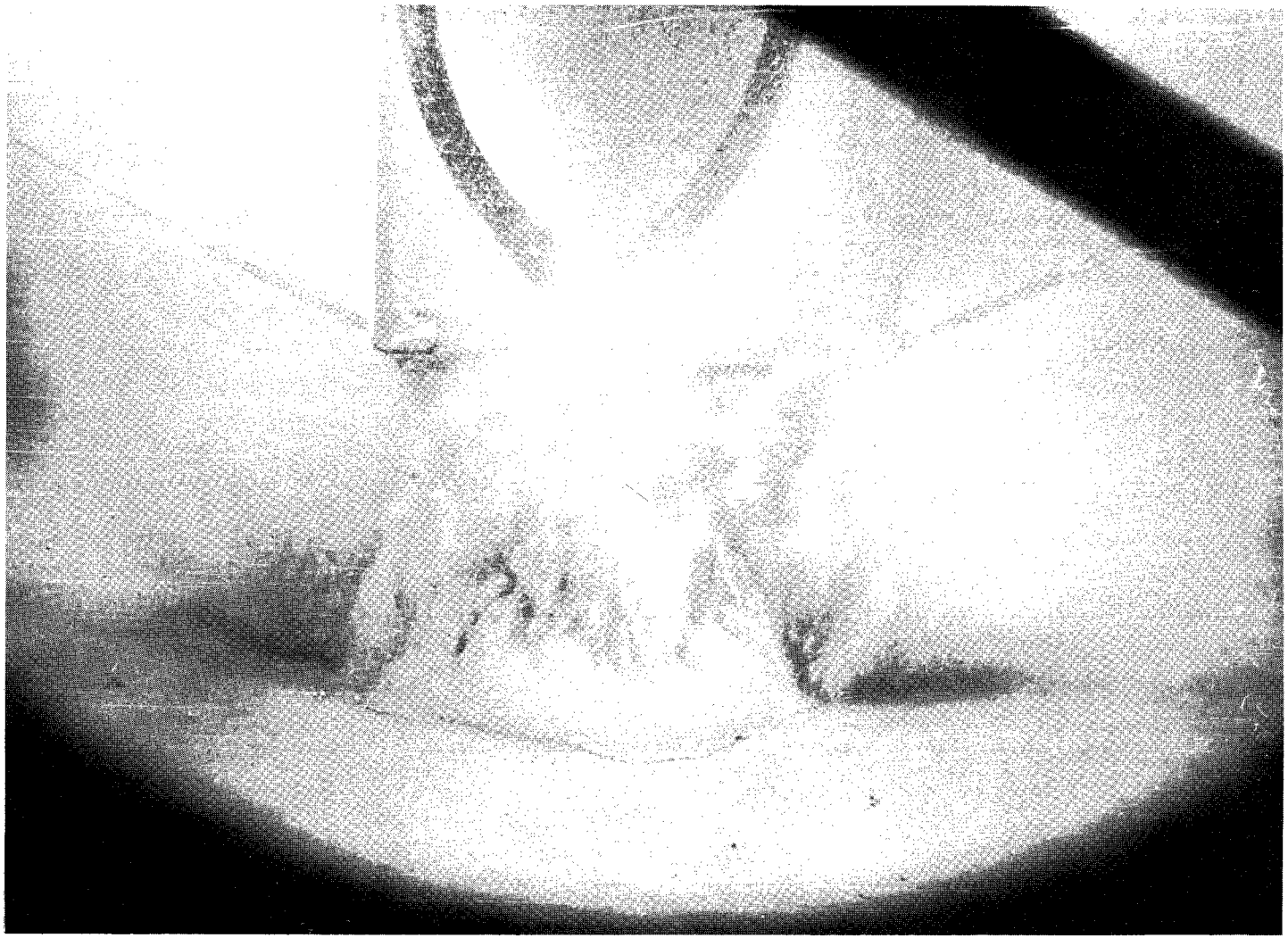

(c) t_o + 0.133 second. L-64-4765

Figure 10.- Continued.

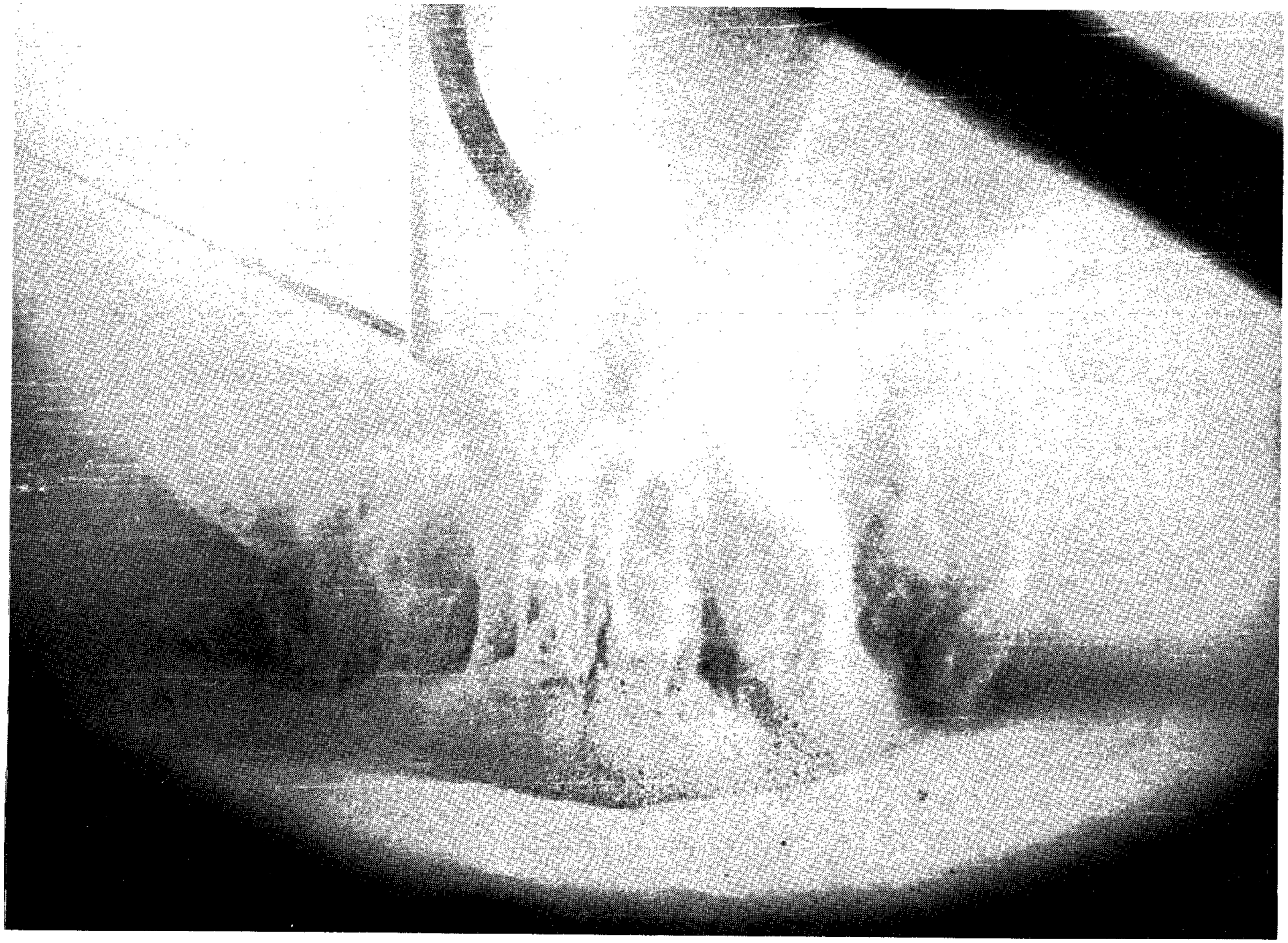

(d) t_o + 0.200 second.

L-64-4766

Figure 10.- Continued.

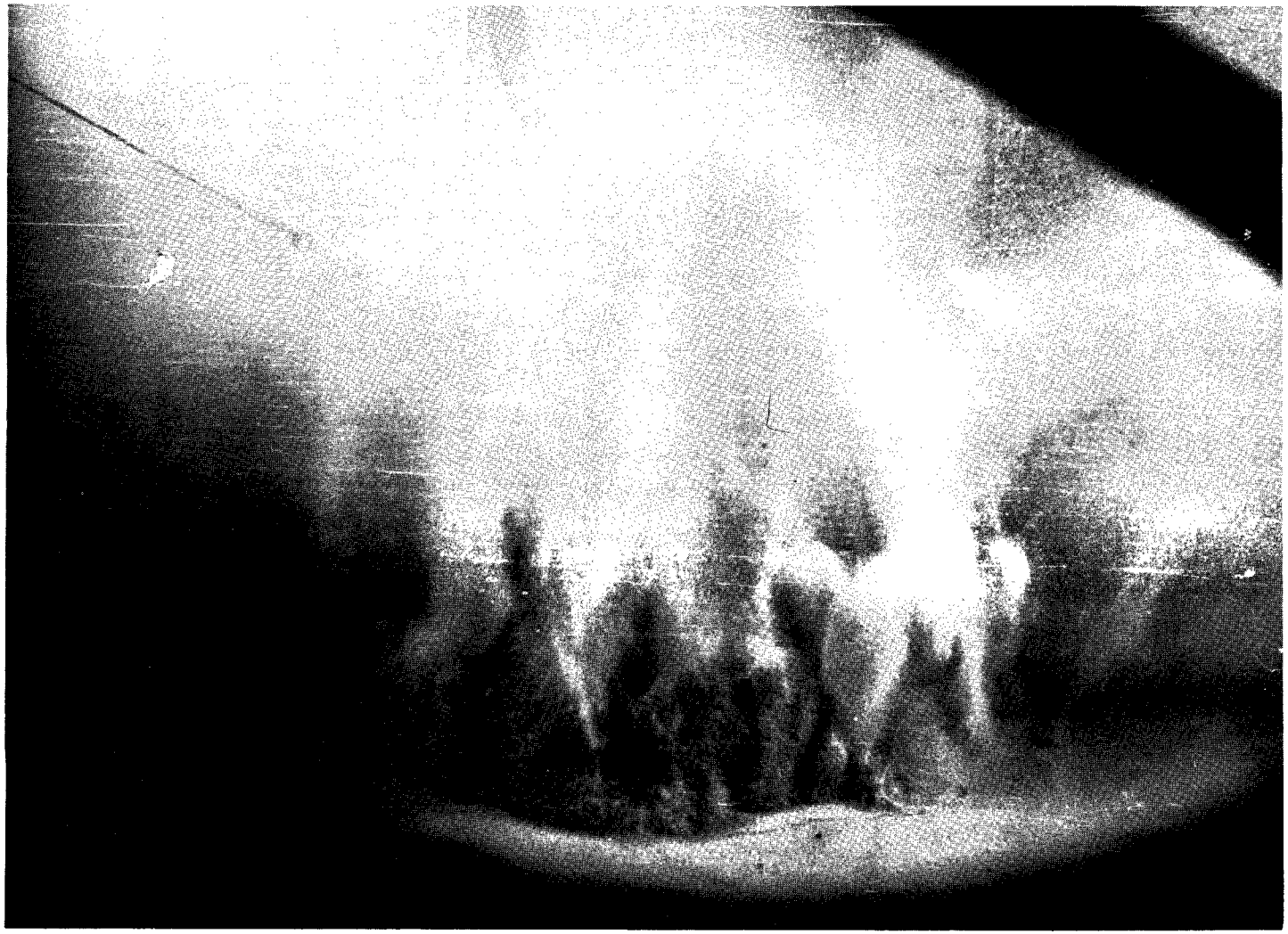

(e) t_o + 0.267 second. L-64-4767

Figure 10.- Continued.

(f) t_o + 0.333 second.

L-64-4768

Figure 10.- Continued.

(g) t_o + 1.000 second.

L-64-4769

Figure 10.- Continued.

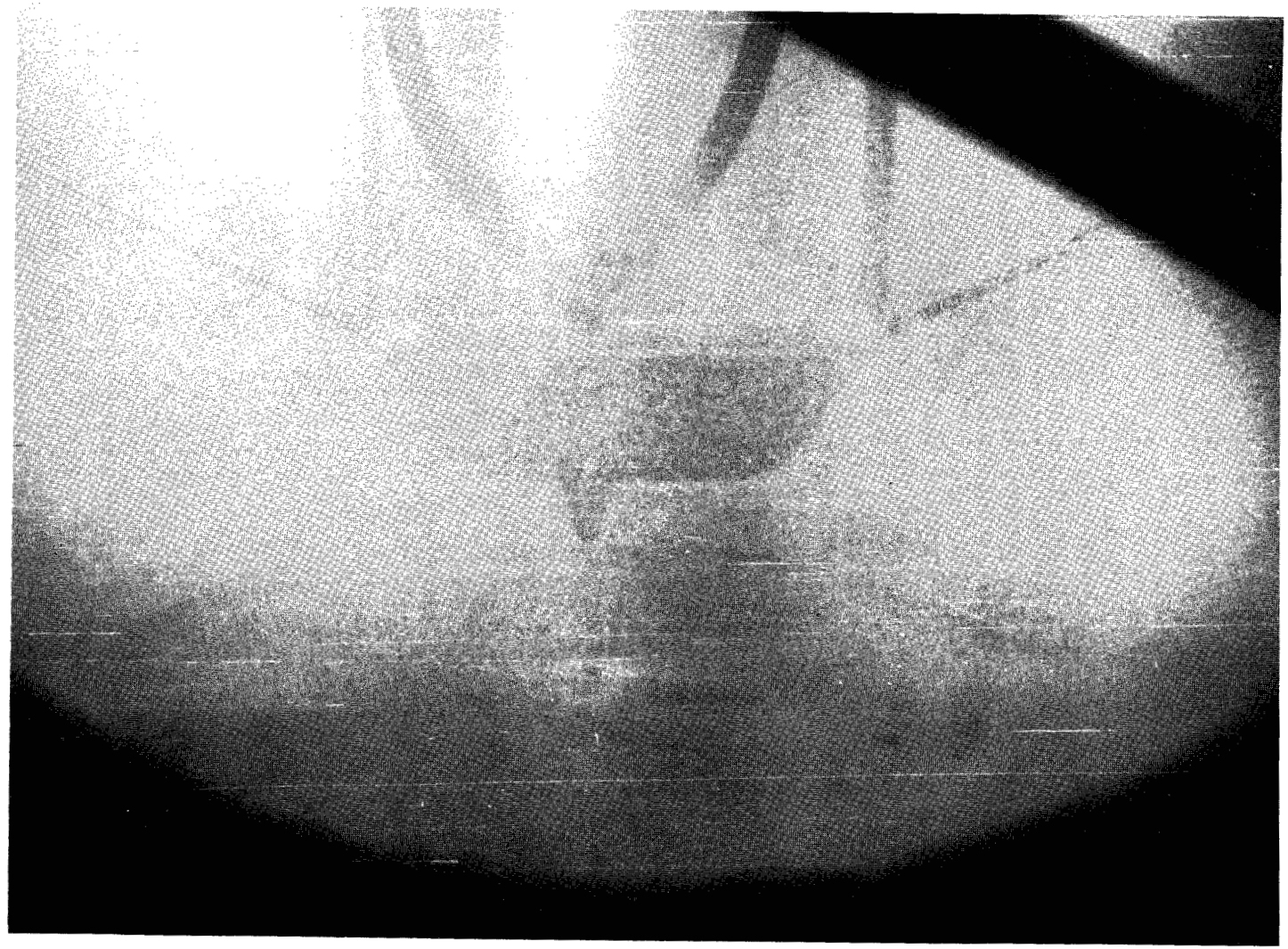

(h) t_o + 10.000 seconds.

L-64-4770

Figure 10.- Concluded.

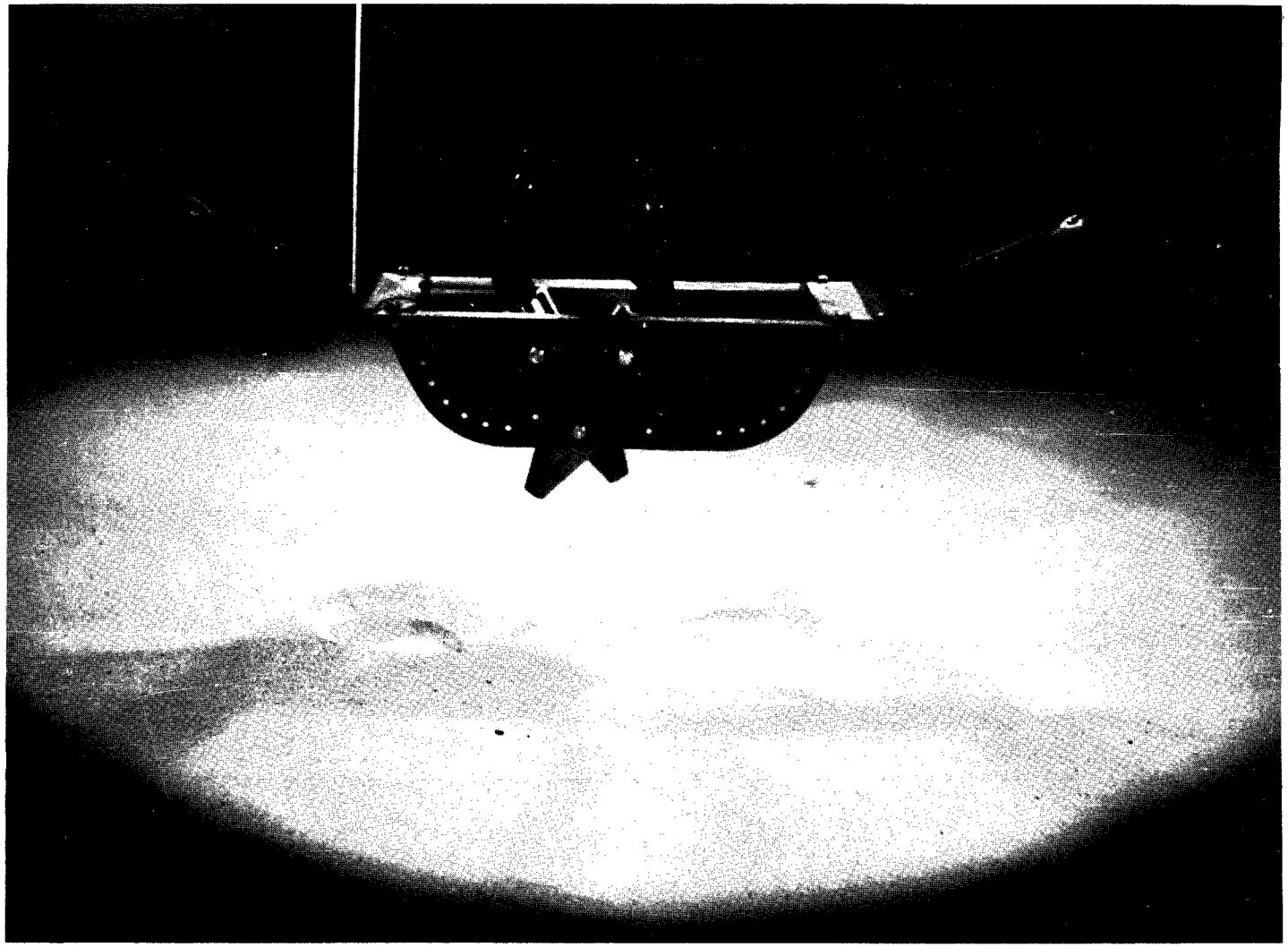

(a) Static conditions. L-64-4771

Figure 11.- Photographic sequence of the twin nozzles. p_∞ = 2 mm Hg; C = 30°; h' = 8 nozzle exit diameters; p_c = 2000 psi; sand-bed depth = 1.6 nozzle diam.

(b) Initial blast, t_o.

L-64-4772

Figure 11.- Continued.

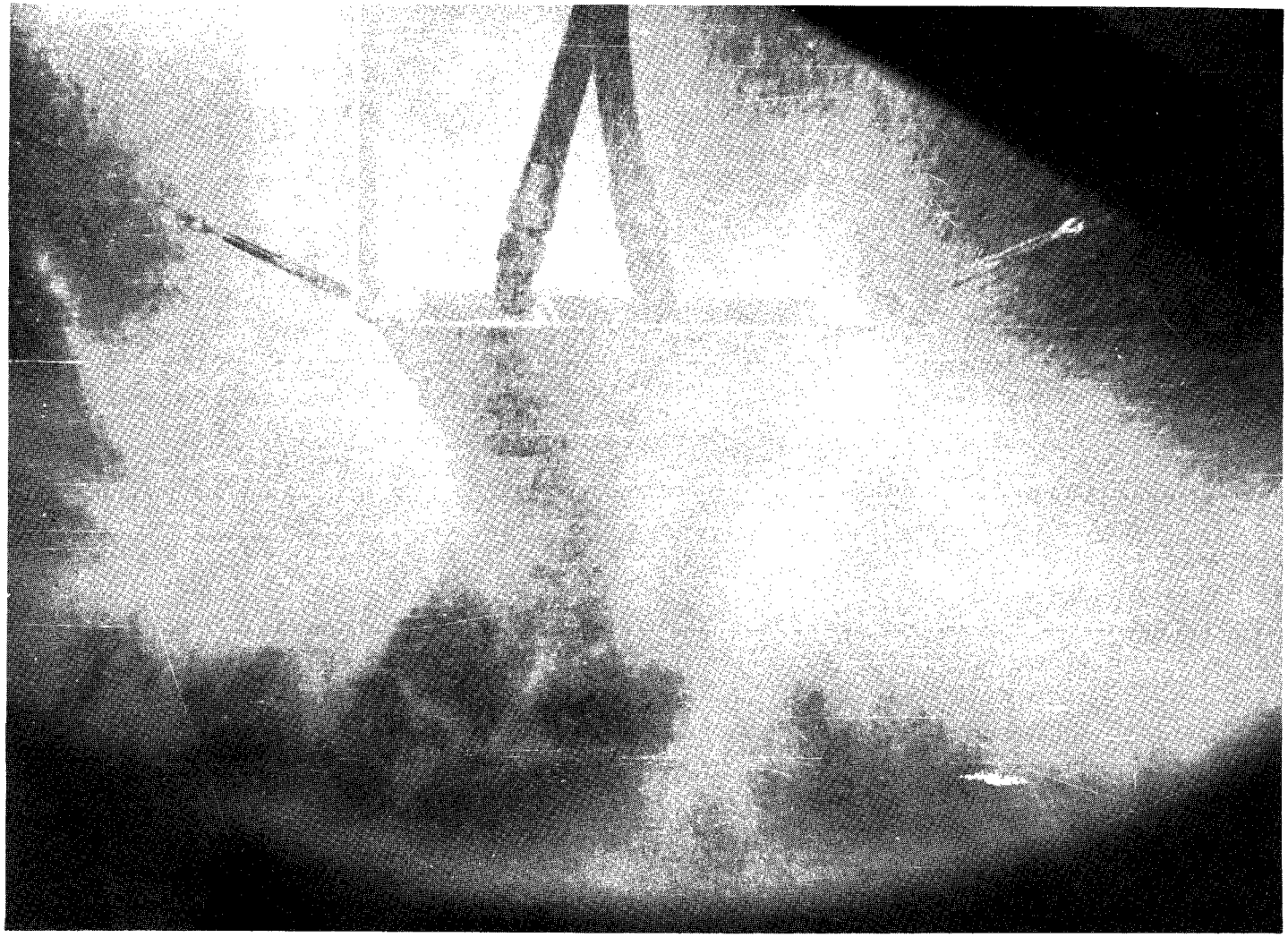

(c) t_o + 0.133 second.

L-64-4773

Figure 11.- Continued.

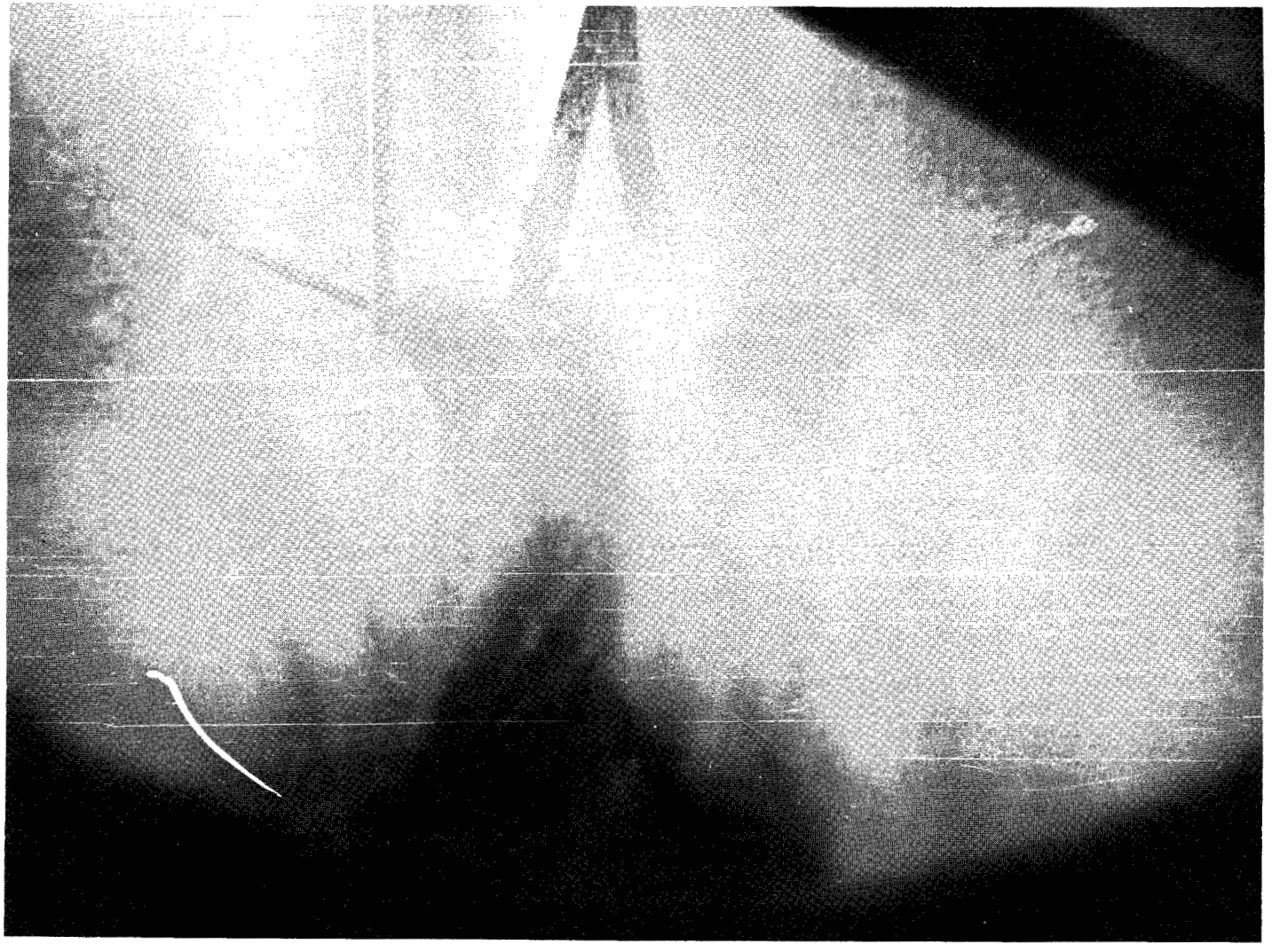

(d) t_o + 0.200 second. L-64-4774

Figure 11.- Continued.

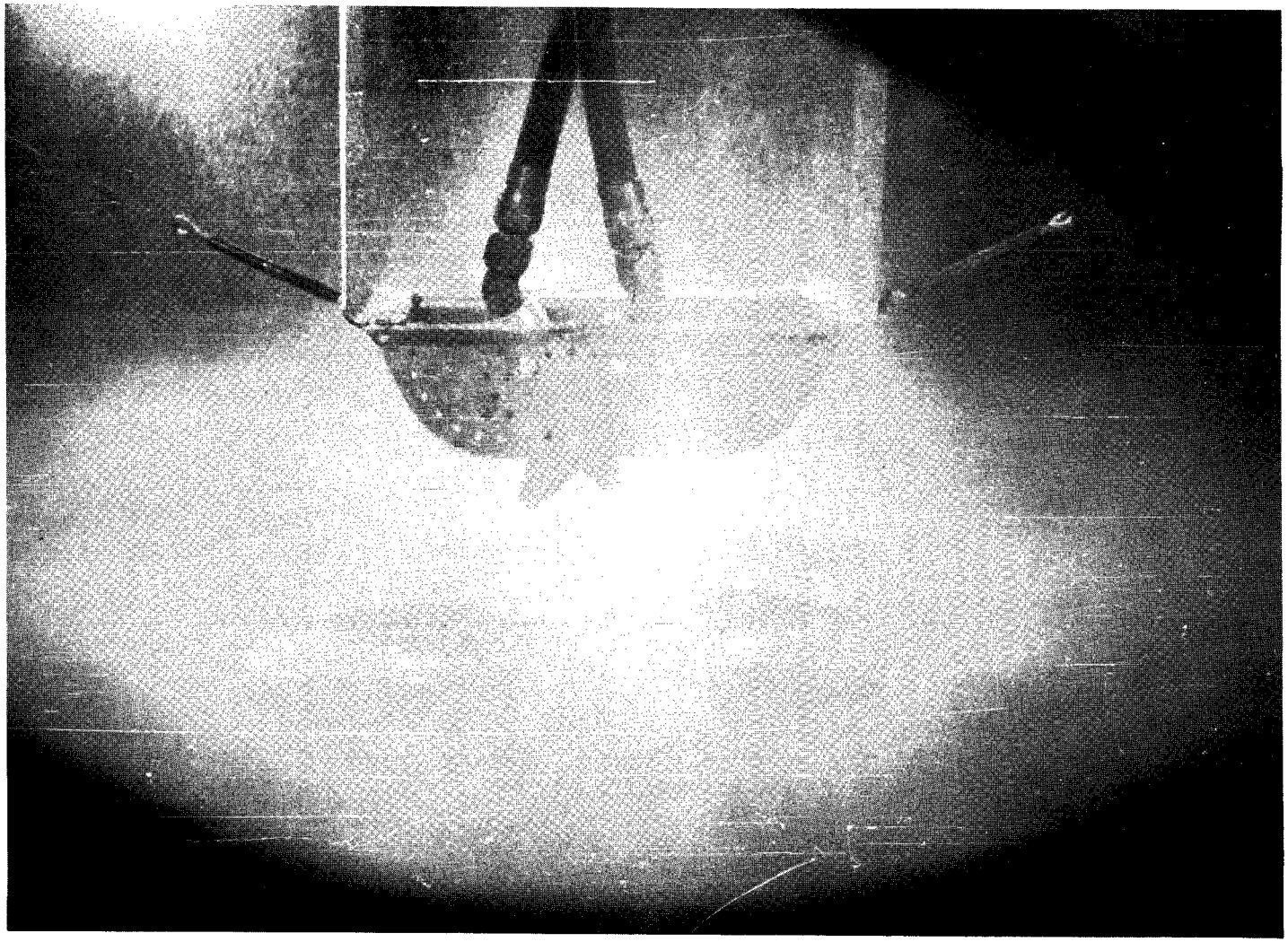

(e) t_o + 0.533 second. L-64-4775

Figure 11.- Continued.

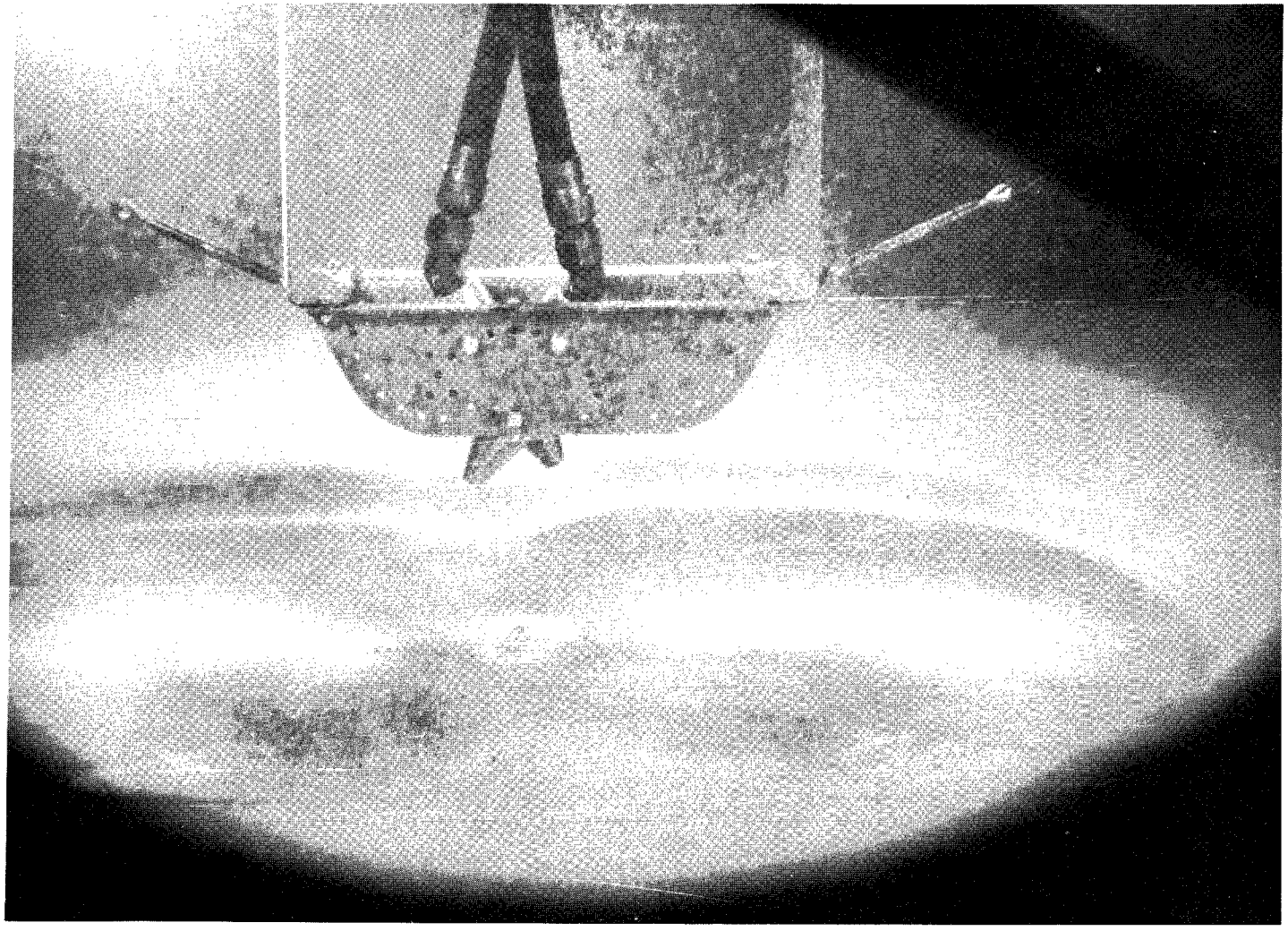

(f) t_o + 10.000 seconds. L-64-4776

Figure 11.- Concluded.

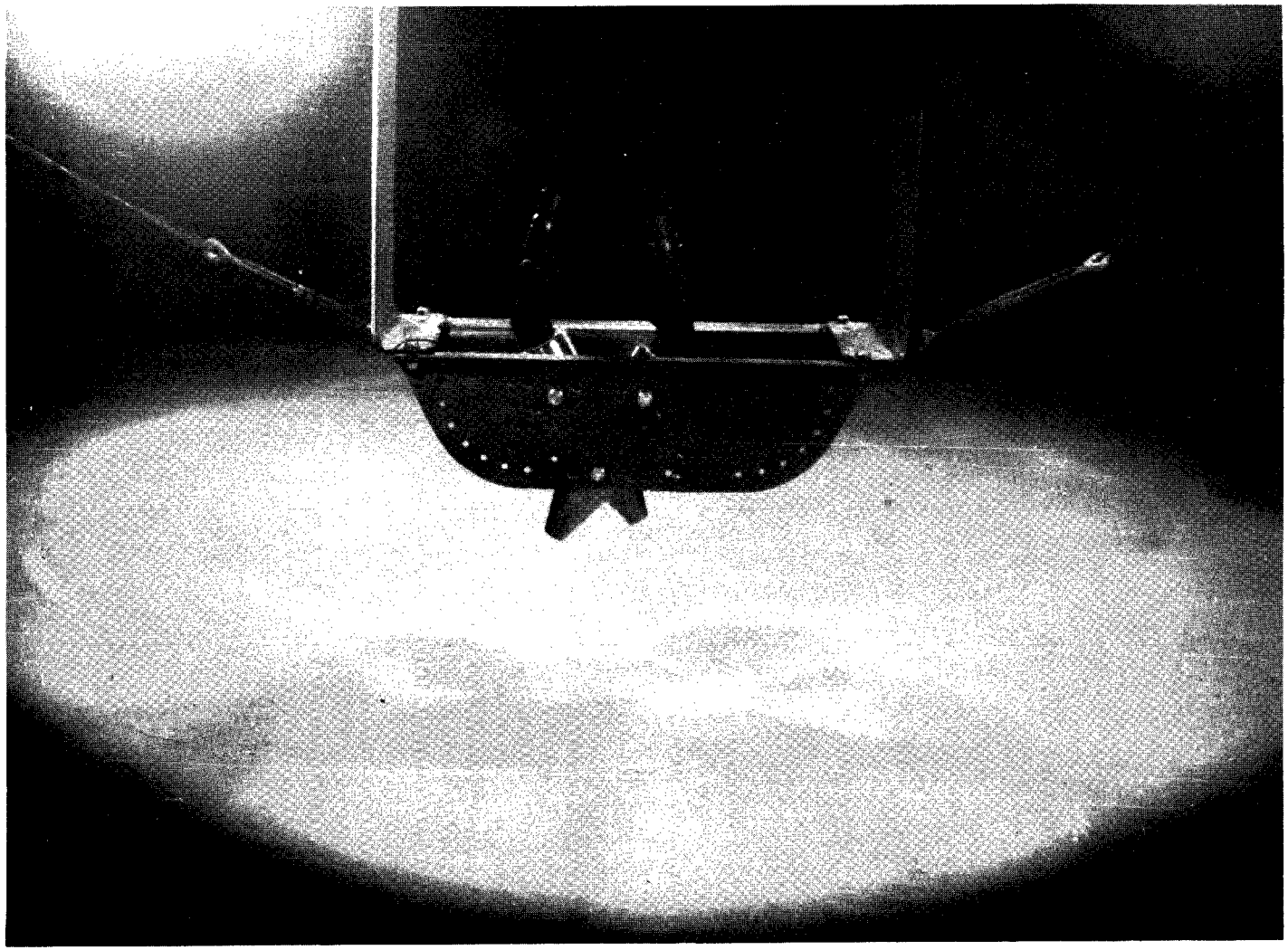

(a) Static conditions. L-64-4777

Figure 12.- Photographic sequence of the twin nozzles. p_∞ = 1 atm; C = 30°; h = 8 nozzle exit diameters; p_c = 2000 psi; sand-bed depth = 1.6 nozzle diam.

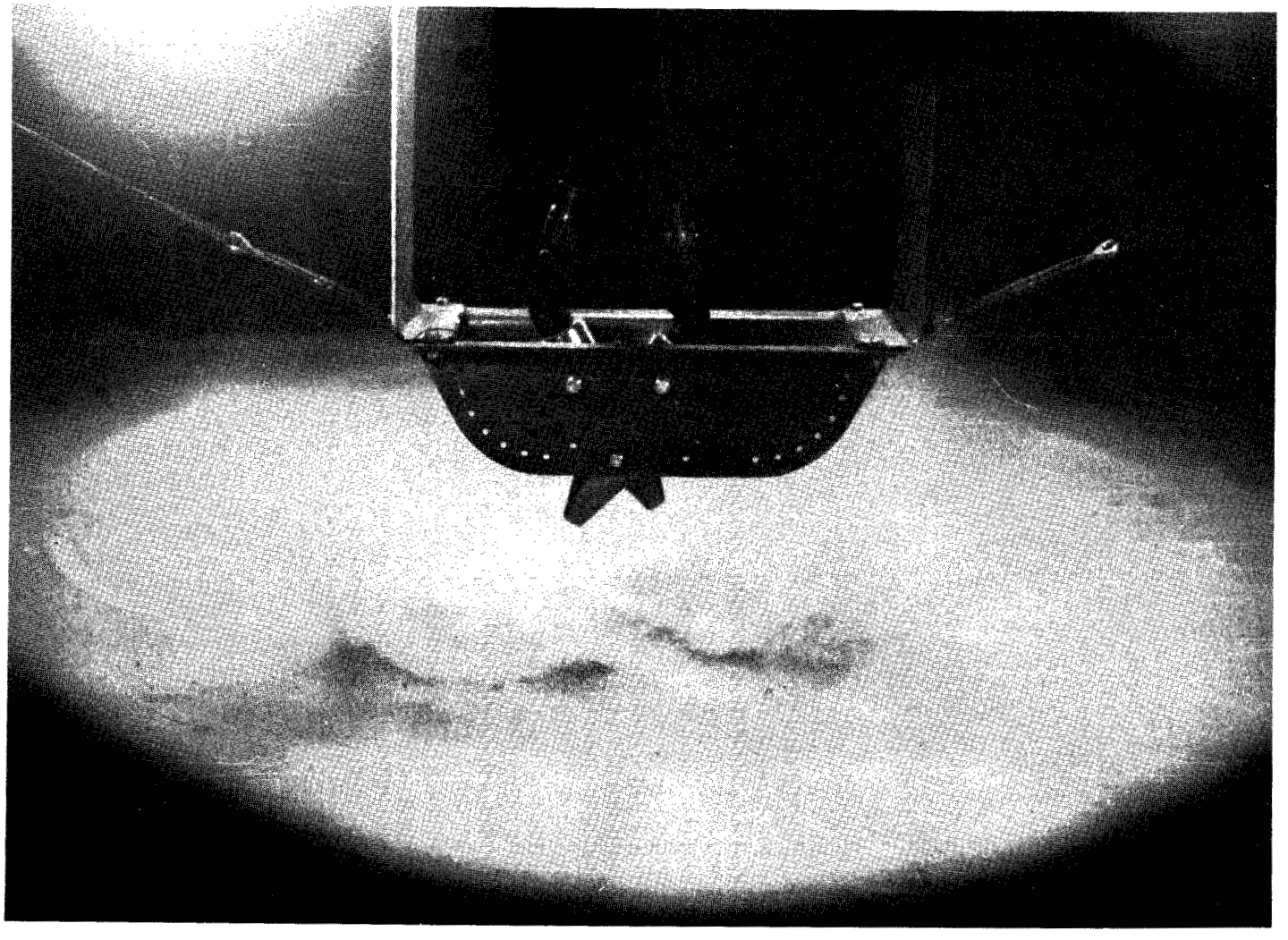

(b) Initial blast, t_o.

L-64-4778

Figure 12.- Continued.

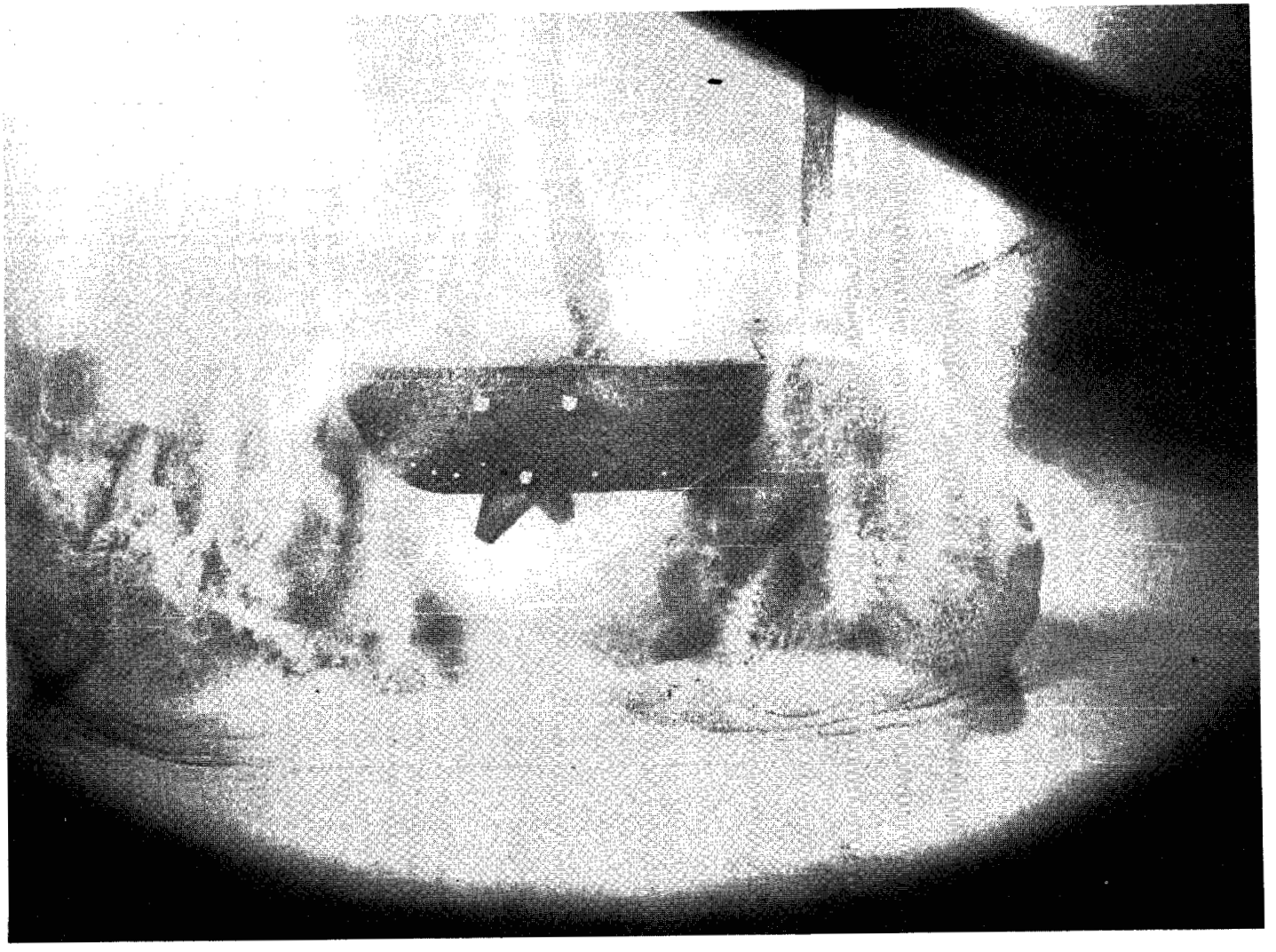

(c) t_o + 0.133 second.

L-64-4779

Figure 12.- Continued.

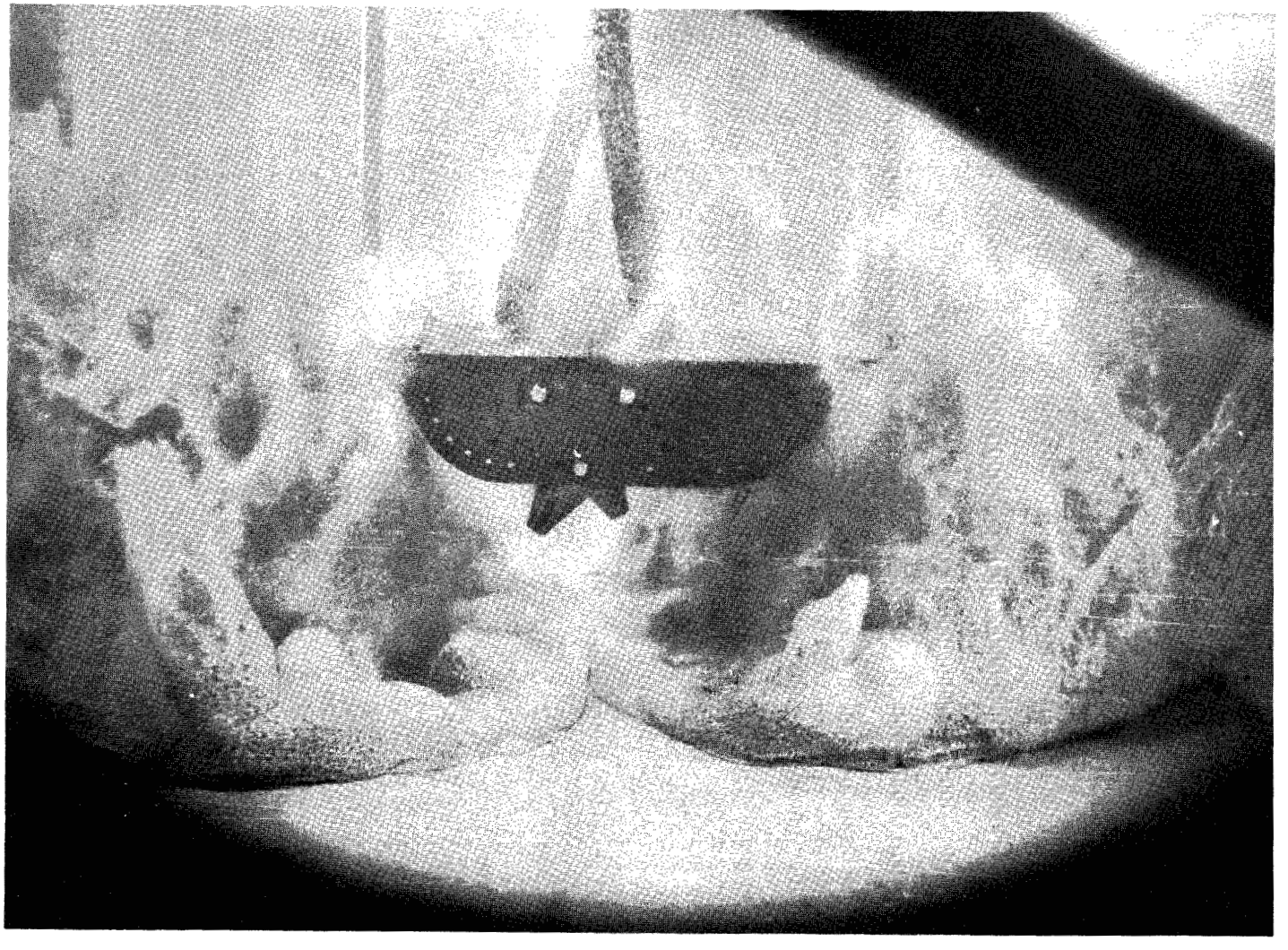

(d) t_o + 0.200 second. L-64-4780

Figure 12.- Continued.

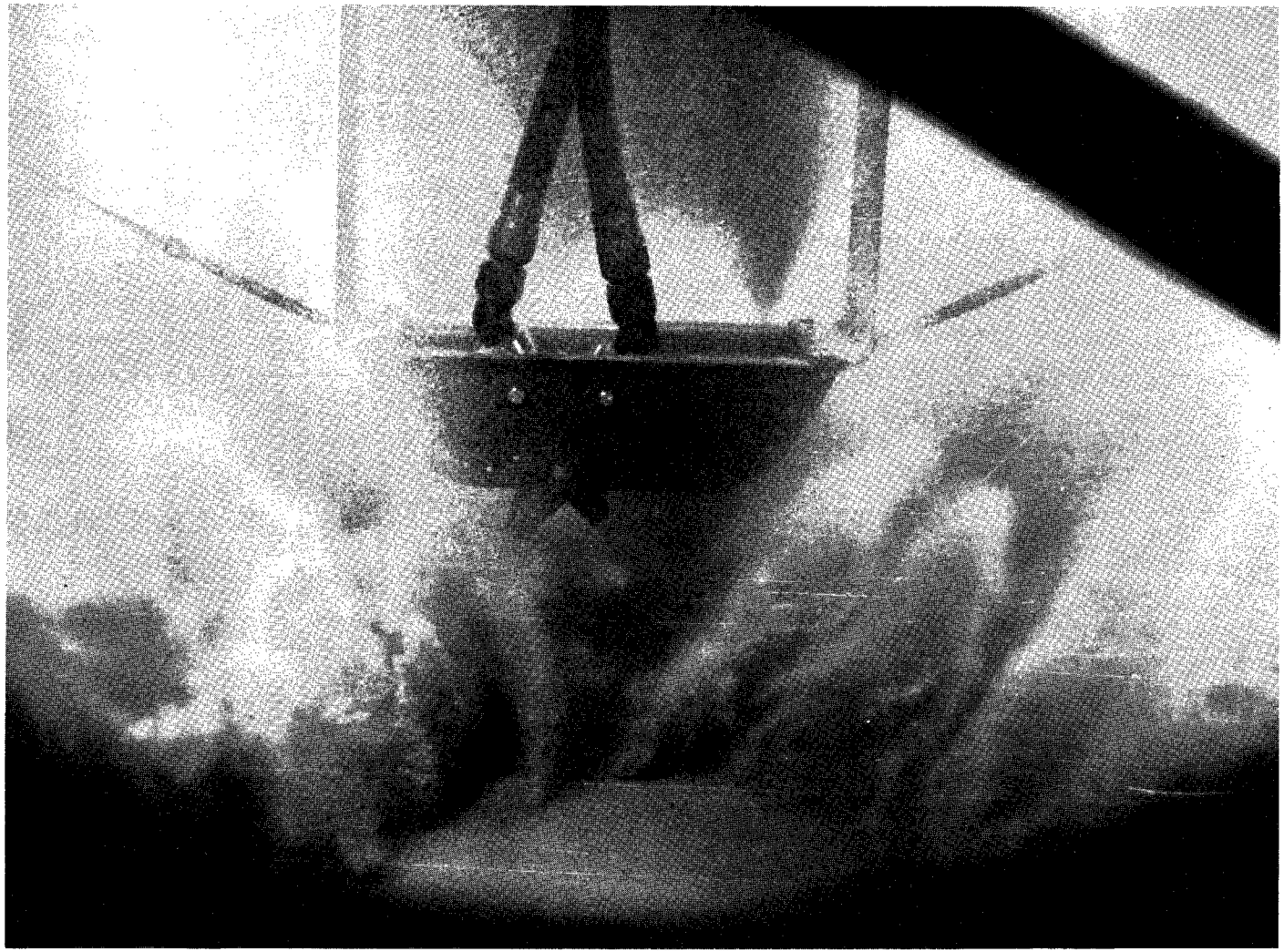

(e) t_o + 0.400 second. L-64-4781

Figure 12.- Continued.

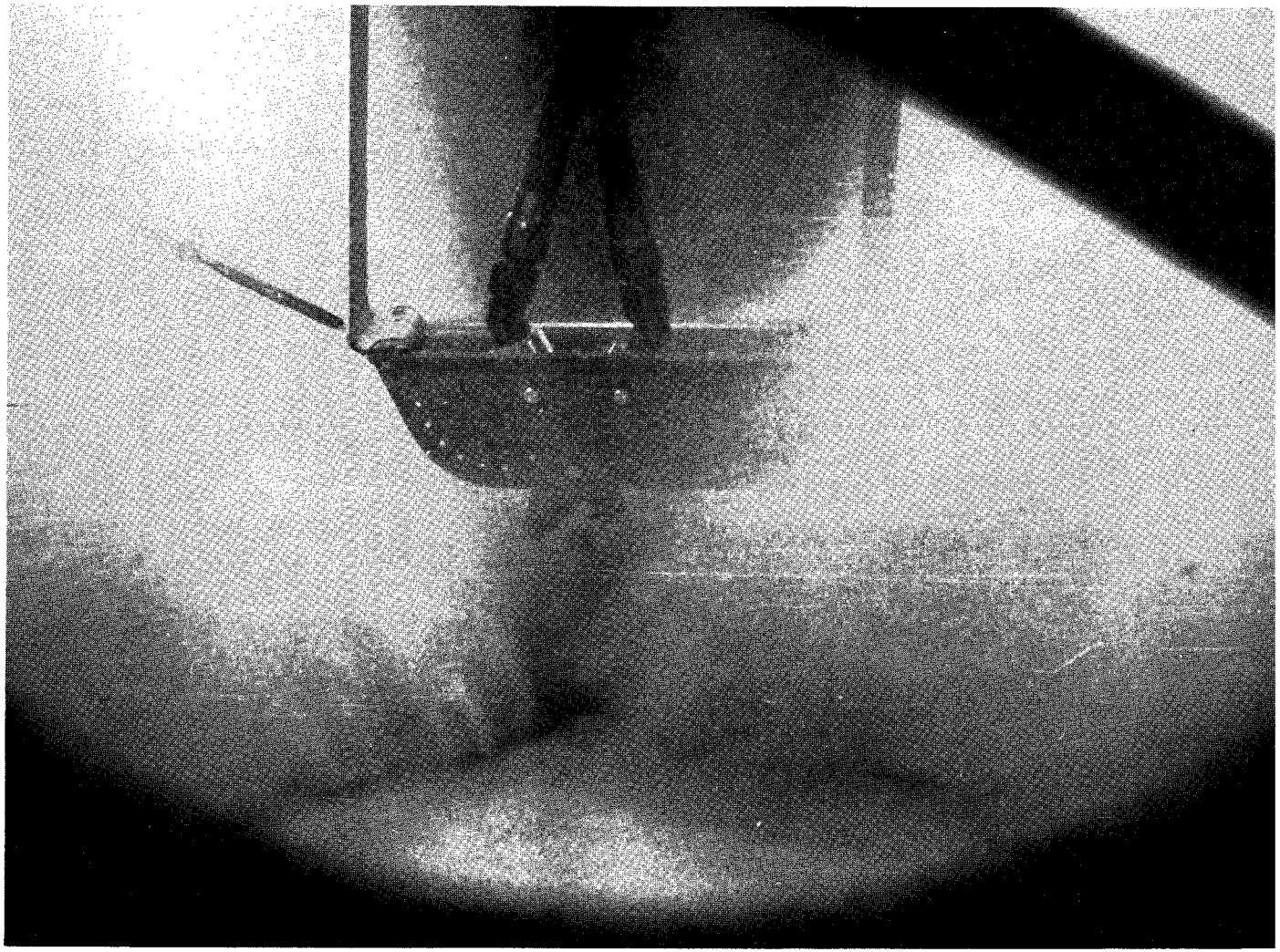

(f) t_o + 1.000 second. L-64-4782

Figure 12.- Continued.

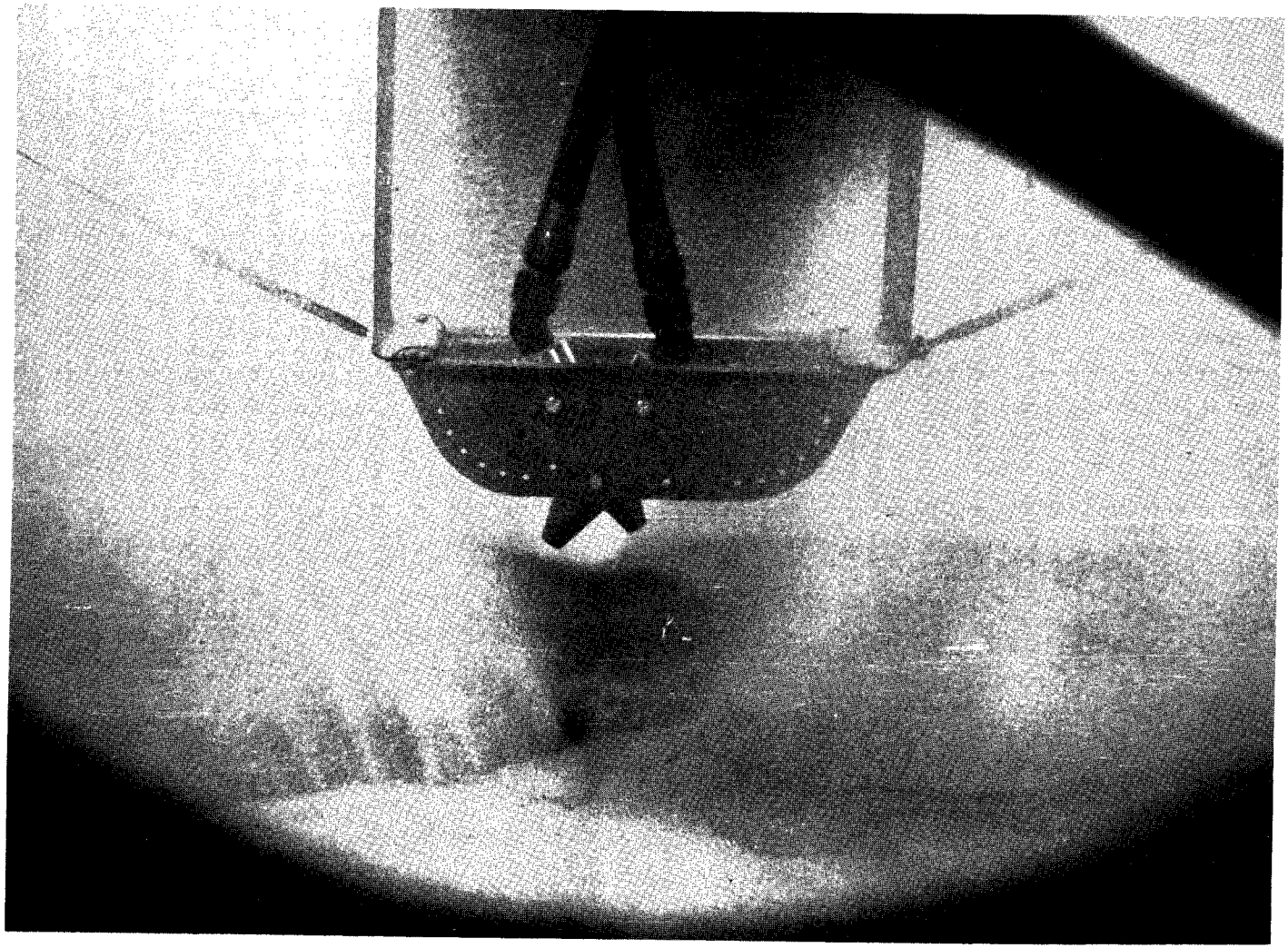

(g) t_o + 1.667 seconds. L-64-4783

Figure 12.- Concluded.

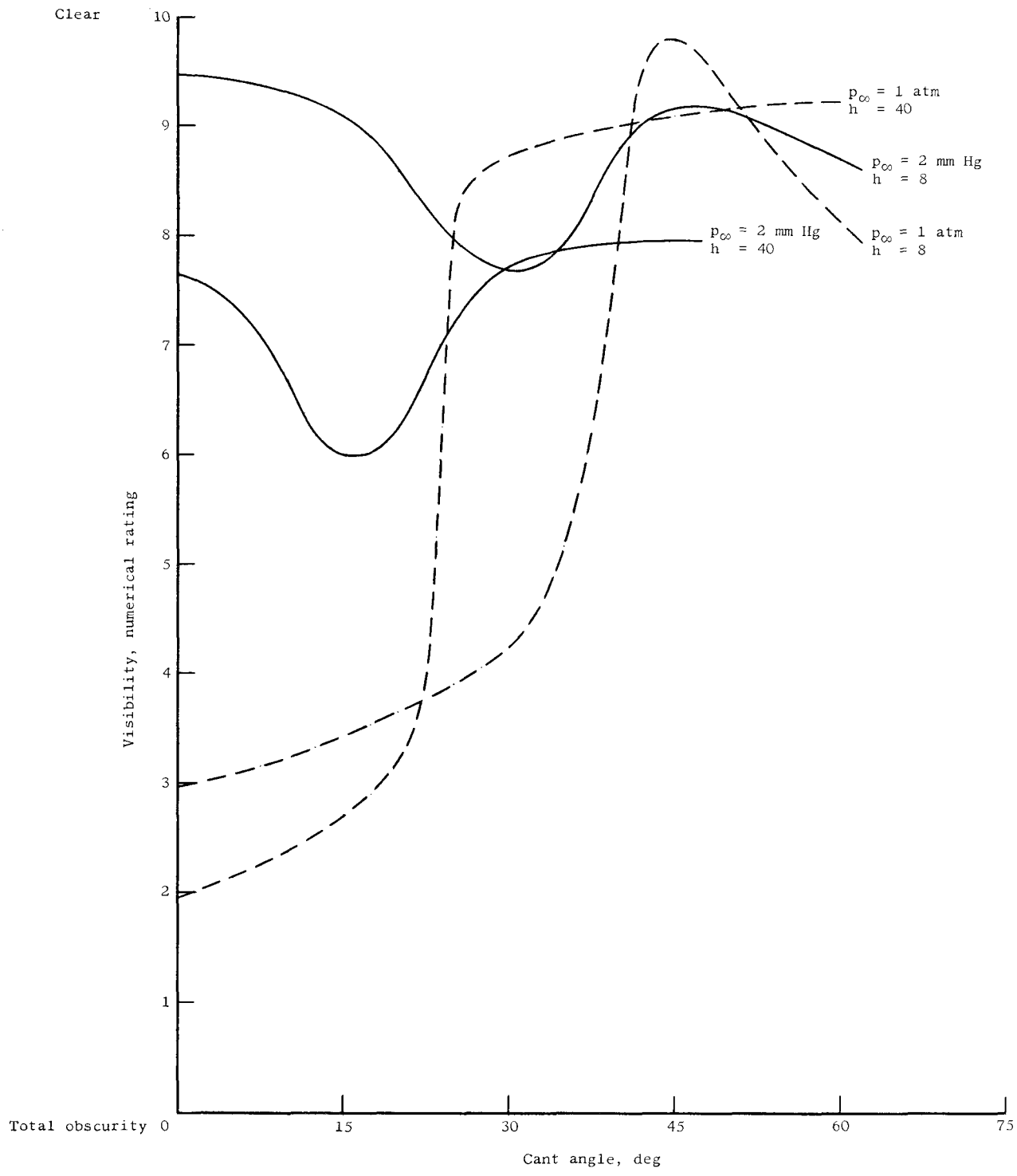

Figure 13.- General trend of the cross-tunnel visibility observed during the tests.

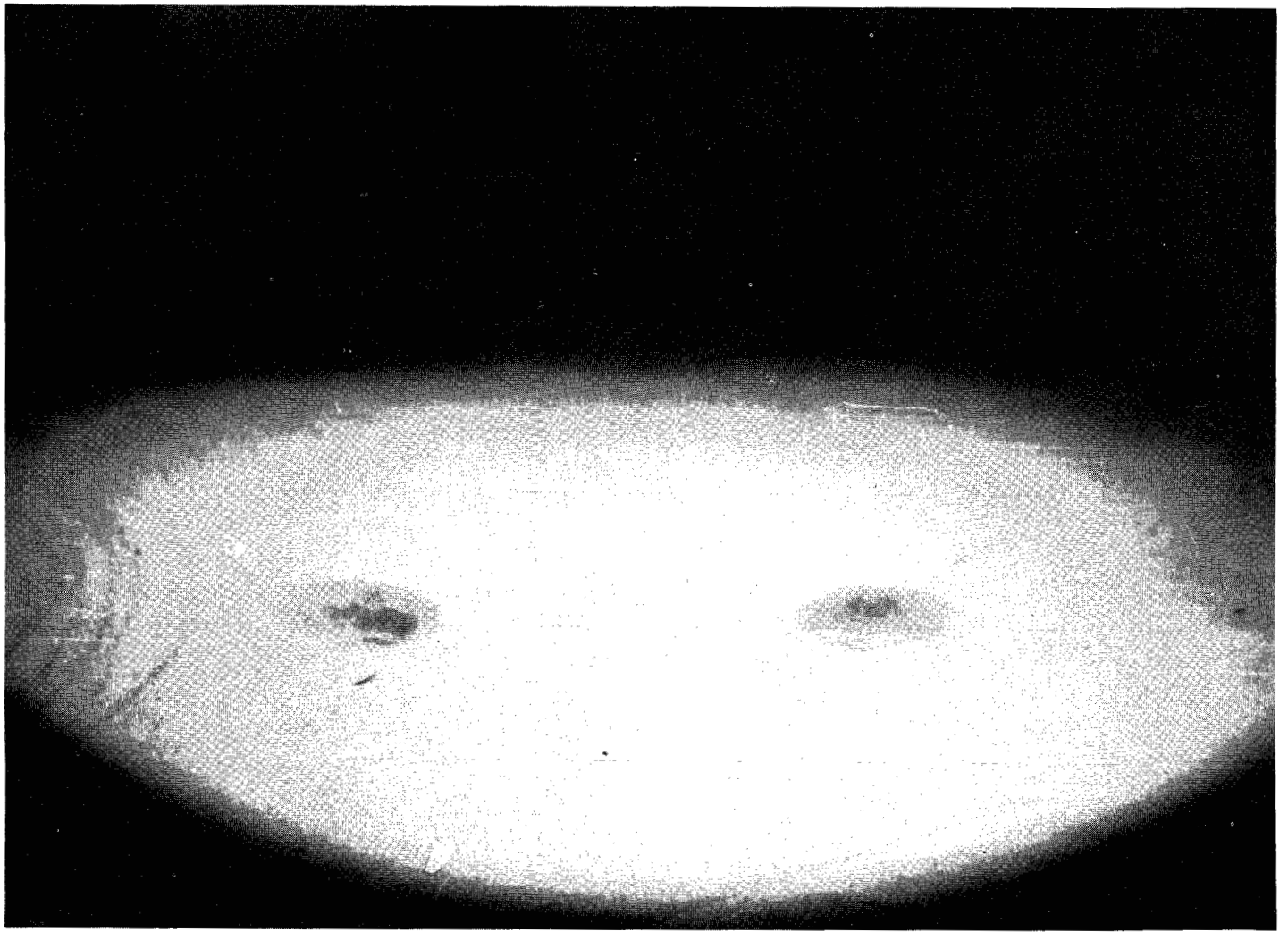

(a) Static conditions.

L-64-4784

Figure 14.- Photographic sequence of the worst combination of conditions for which the twin nozzles were tested. p_∞ = 2 mm Hg; C = 15°; h = 40 nozzle exit diameters; p_c = 2000 psi; sand-bed depth = 1.6 nozzle diam.

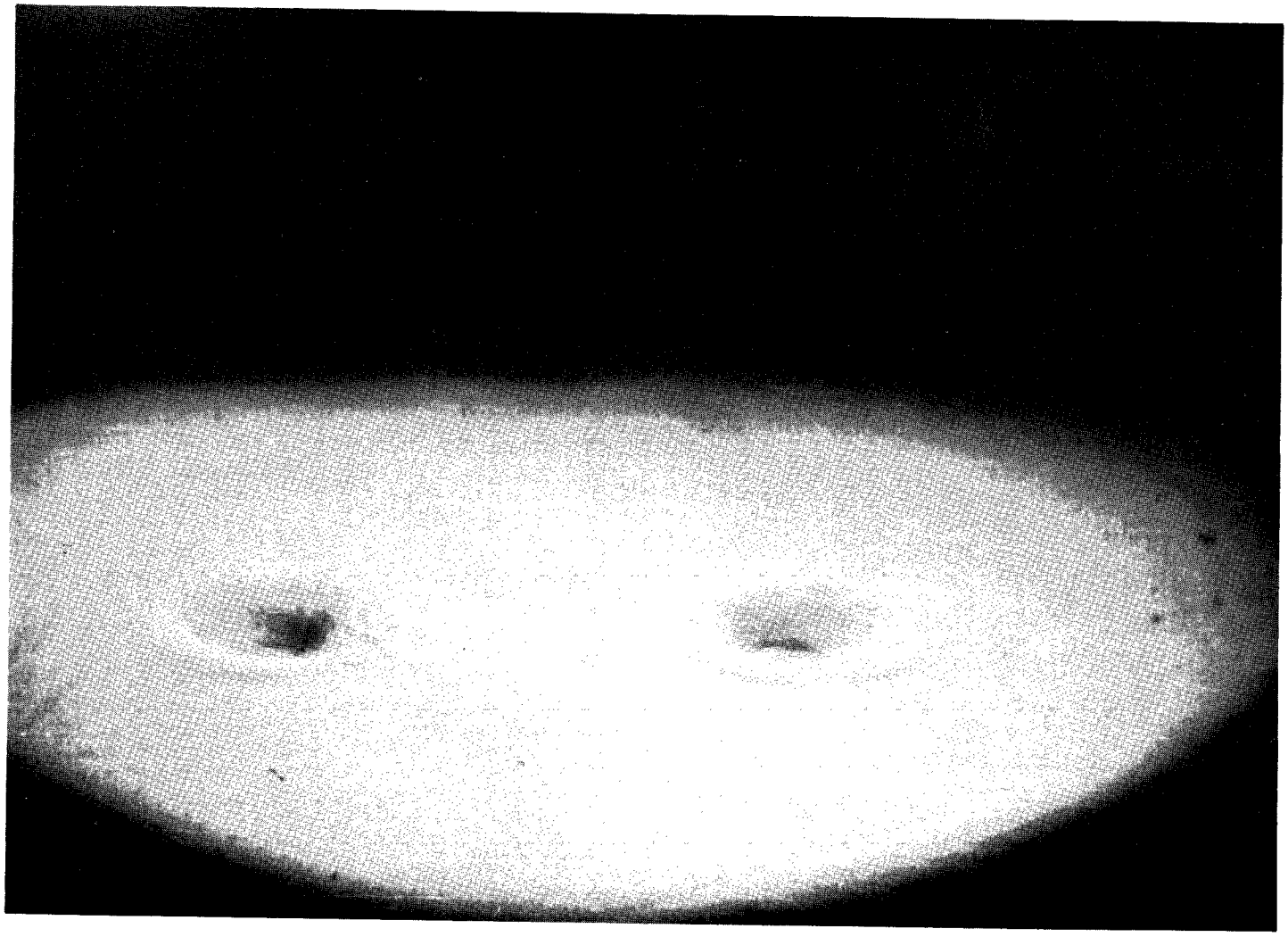

(b) Initial blast, t_o.

L-64-4785

Figure 14.- Continued.

(c) t_o + 0.600 second.

L-64-4786

Figure 14.- Continued.

(d) t_o + 0.867 second. L-64-4787

Figure 14.- Continued.

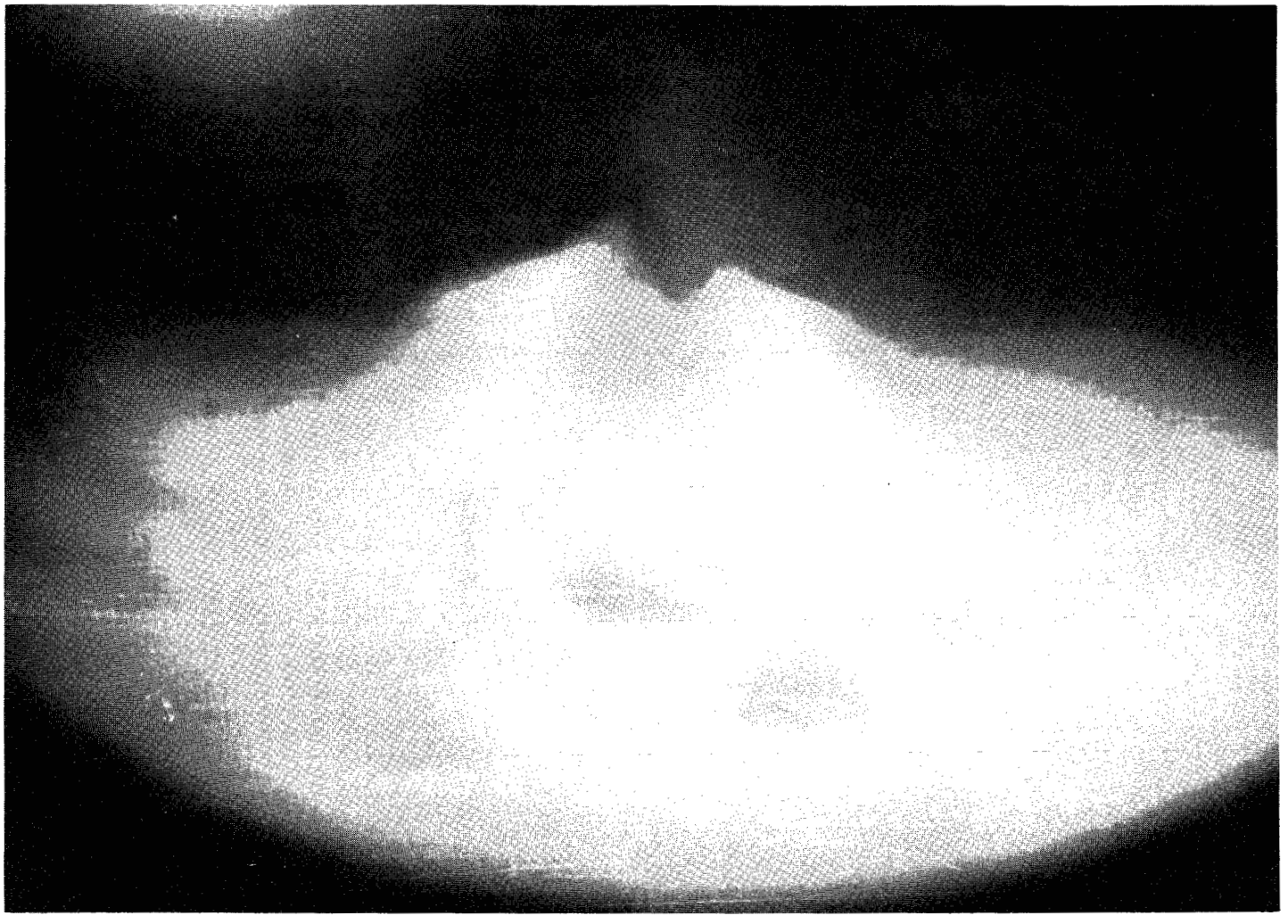

(e) t_o + 1.067 seconds. L-64-4788

Figure 14.- Continued.

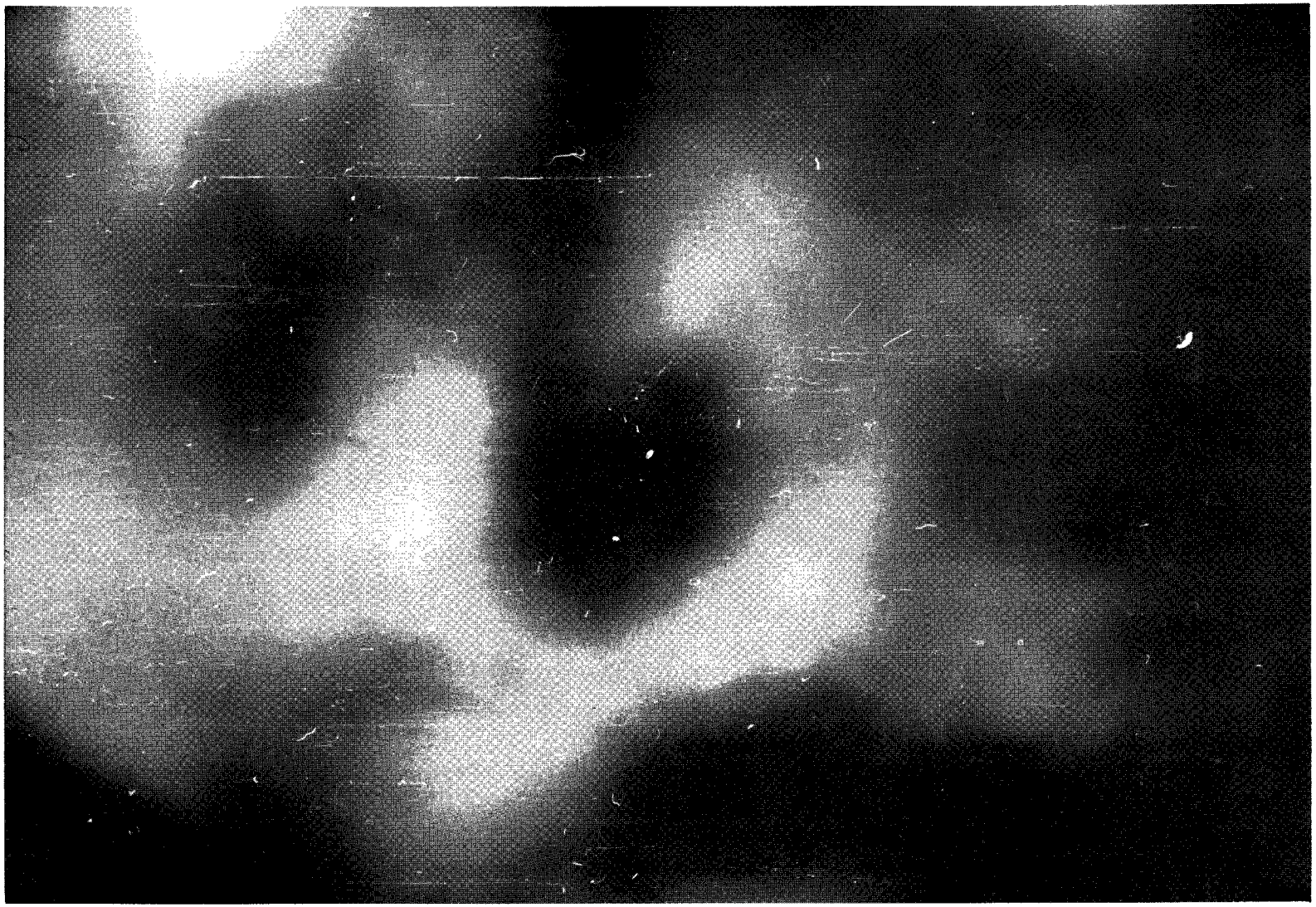

(f) t_o + 1.667 seconds. L-64-4789

Figure 14.- Continued.

(g) t_o + 2.067 seconds. L-64-4790

Figure 14.- Continued.

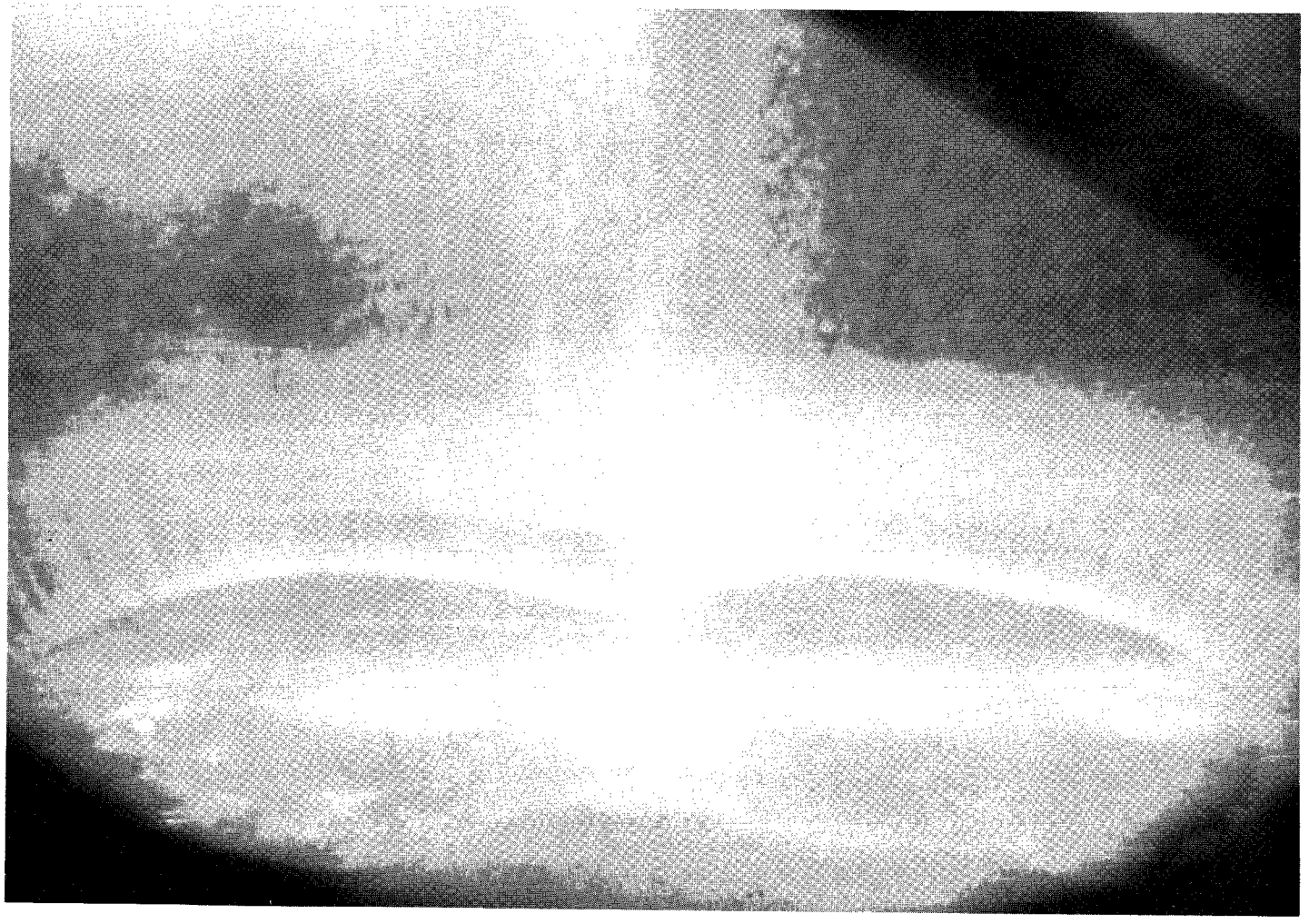

(h) t_o + 10.000 seconds. L-64-4791

Figure 14.- Concluded.

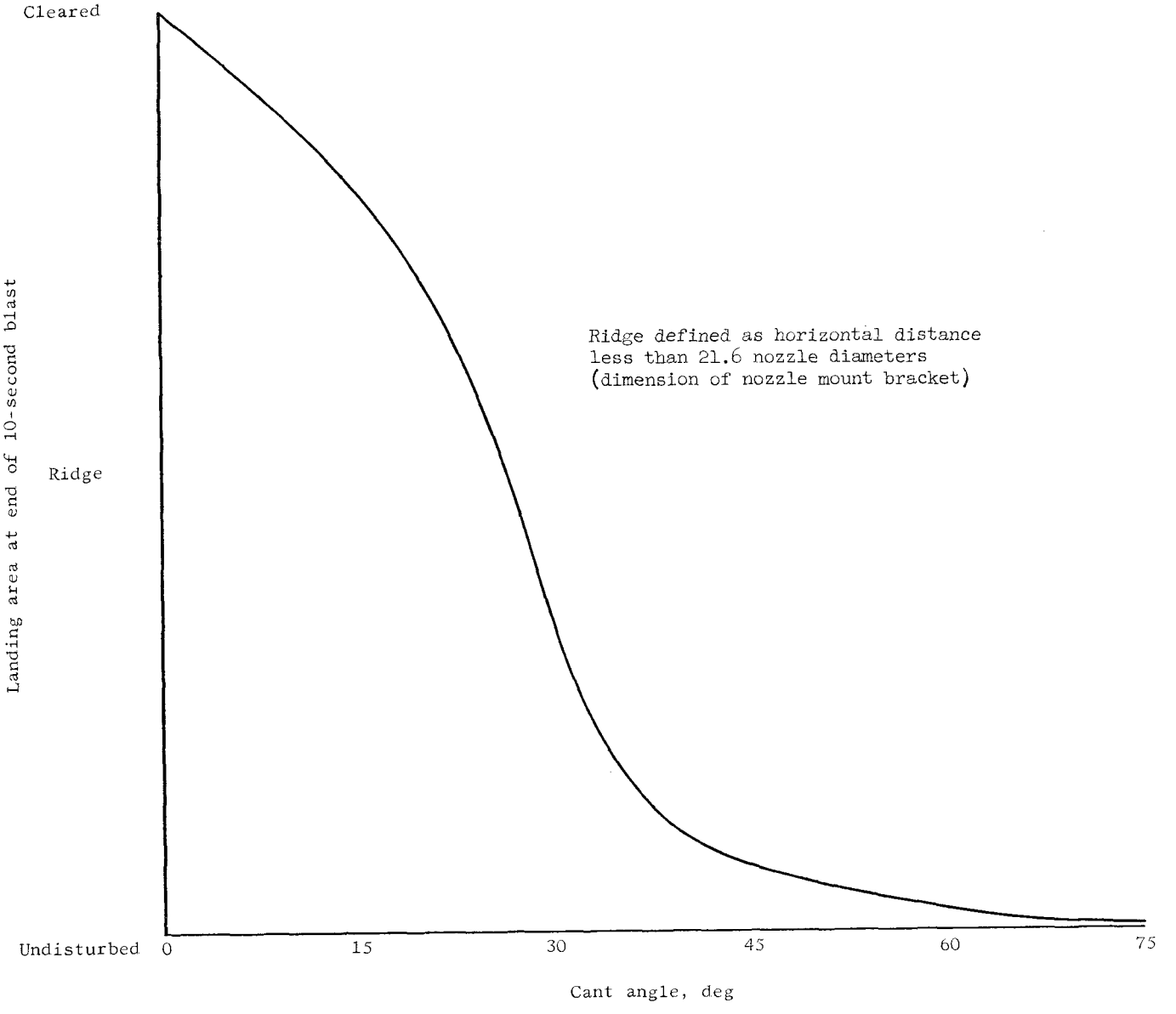

Figure 15.- Trend of blast effect on surface directly under nozzles.

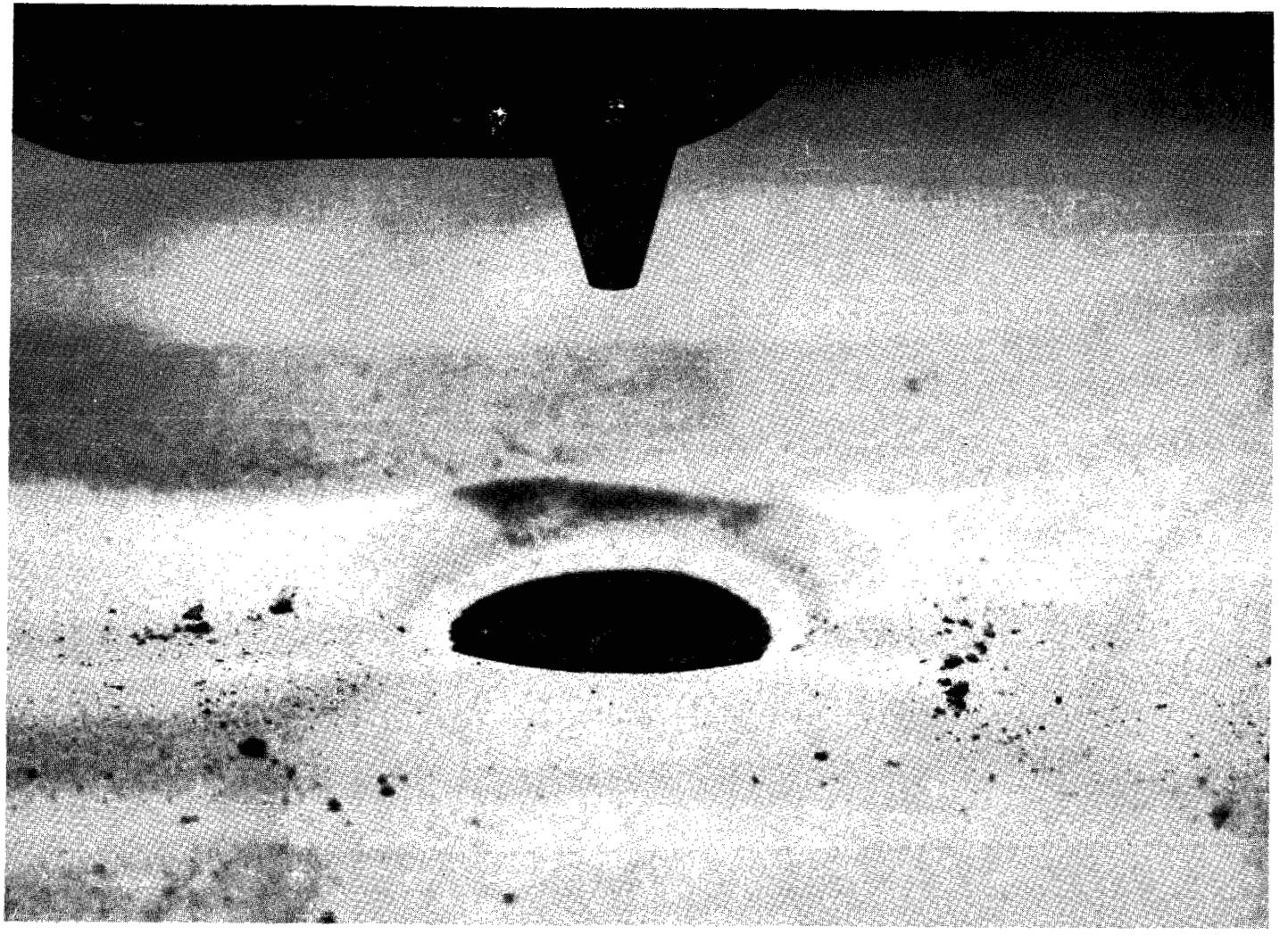

(a) Static conditions.

L-64-4792

Figure 16.- Photographic sequence of a single nozzle. p_∞ = 2 mm Hg; C = 0°; h = 8 nozzle exit diameters; p_c = 2000 psi; sand-bed depth = 1.6 nozzle diam.

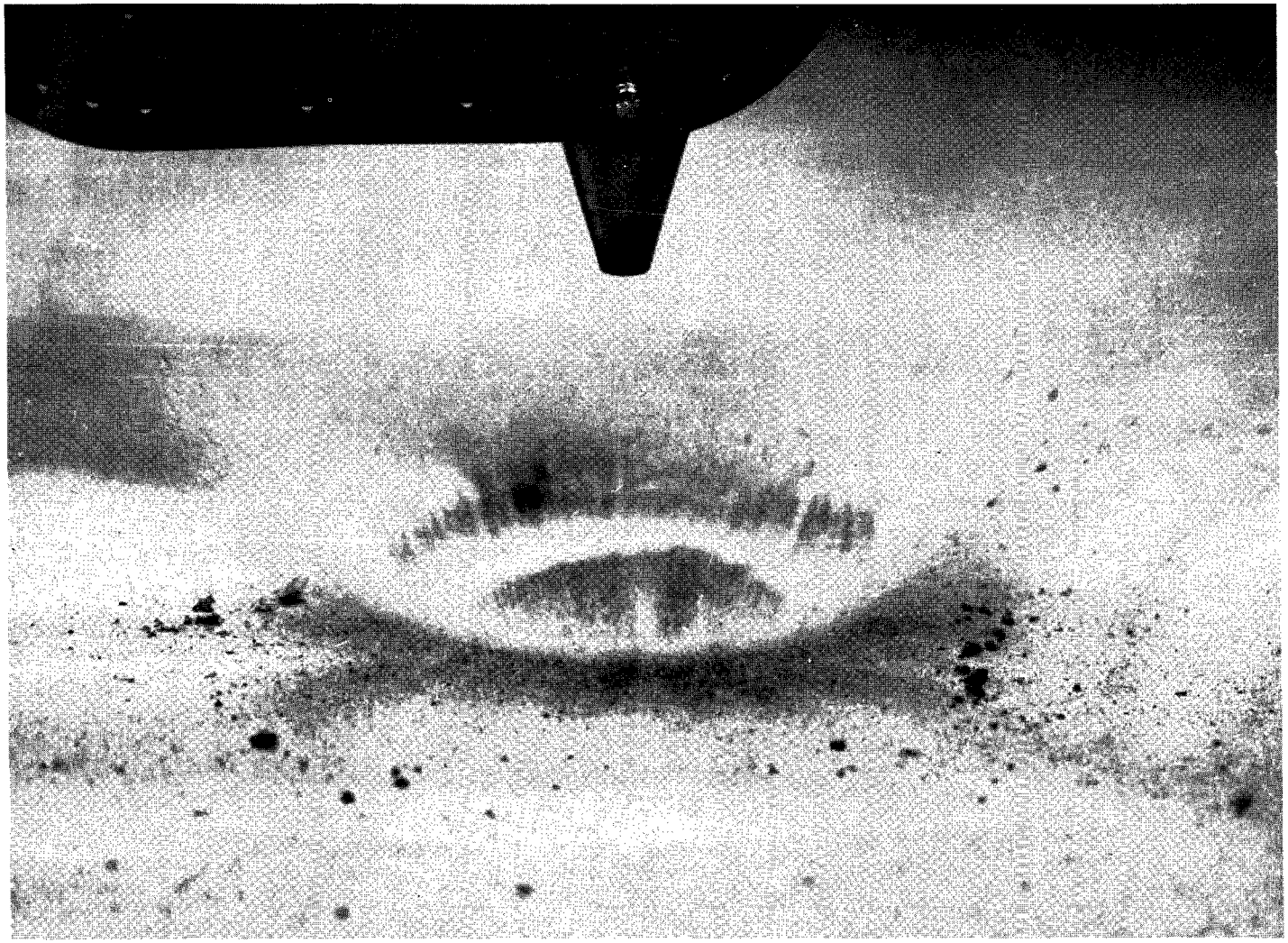

(b) Initial blast, t_o. L-64-4793

Figure 16.- Continued.

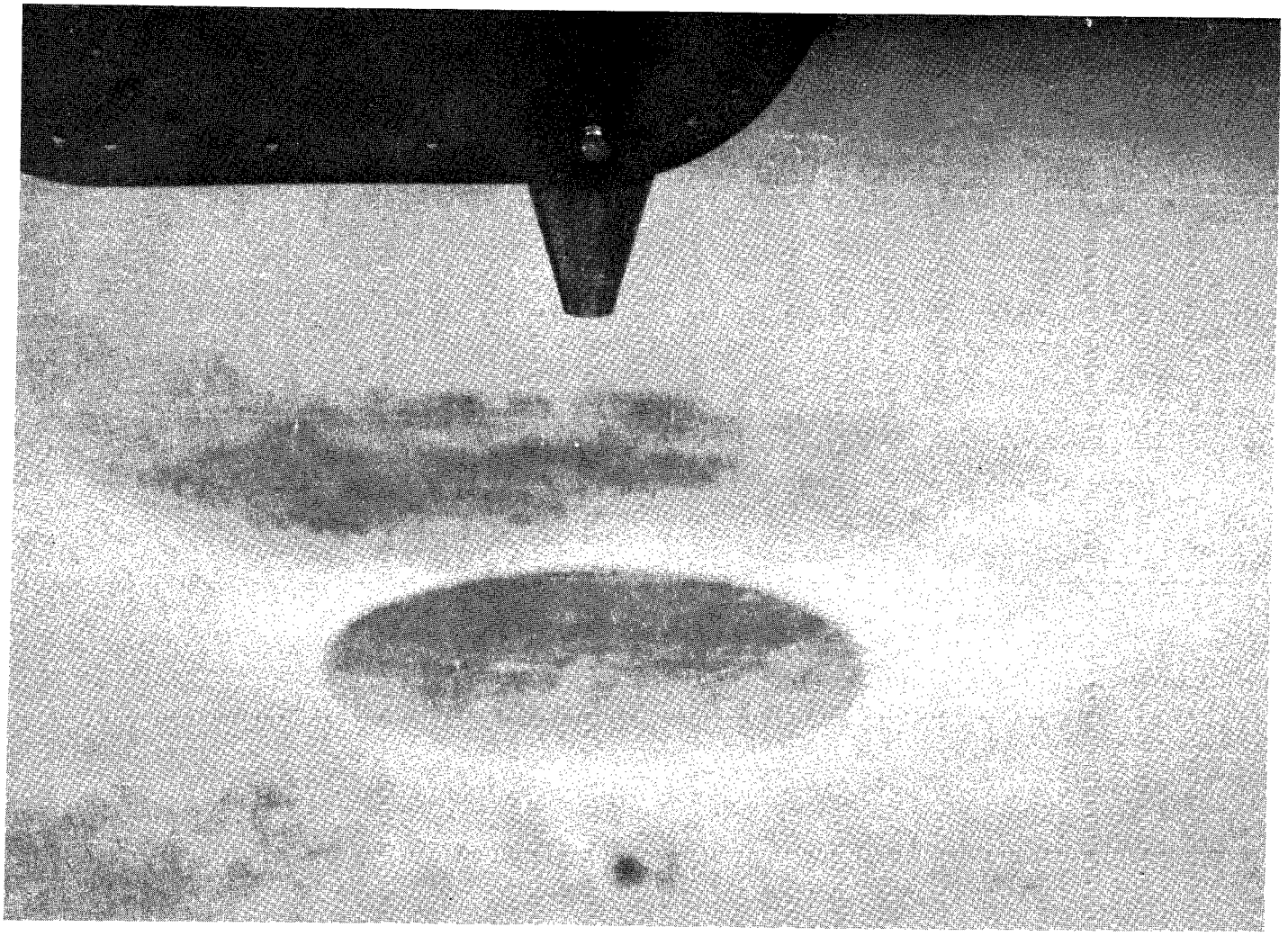

(c) t_o + 0.133 second.

L-64-4794

Figure 16.- Continued.

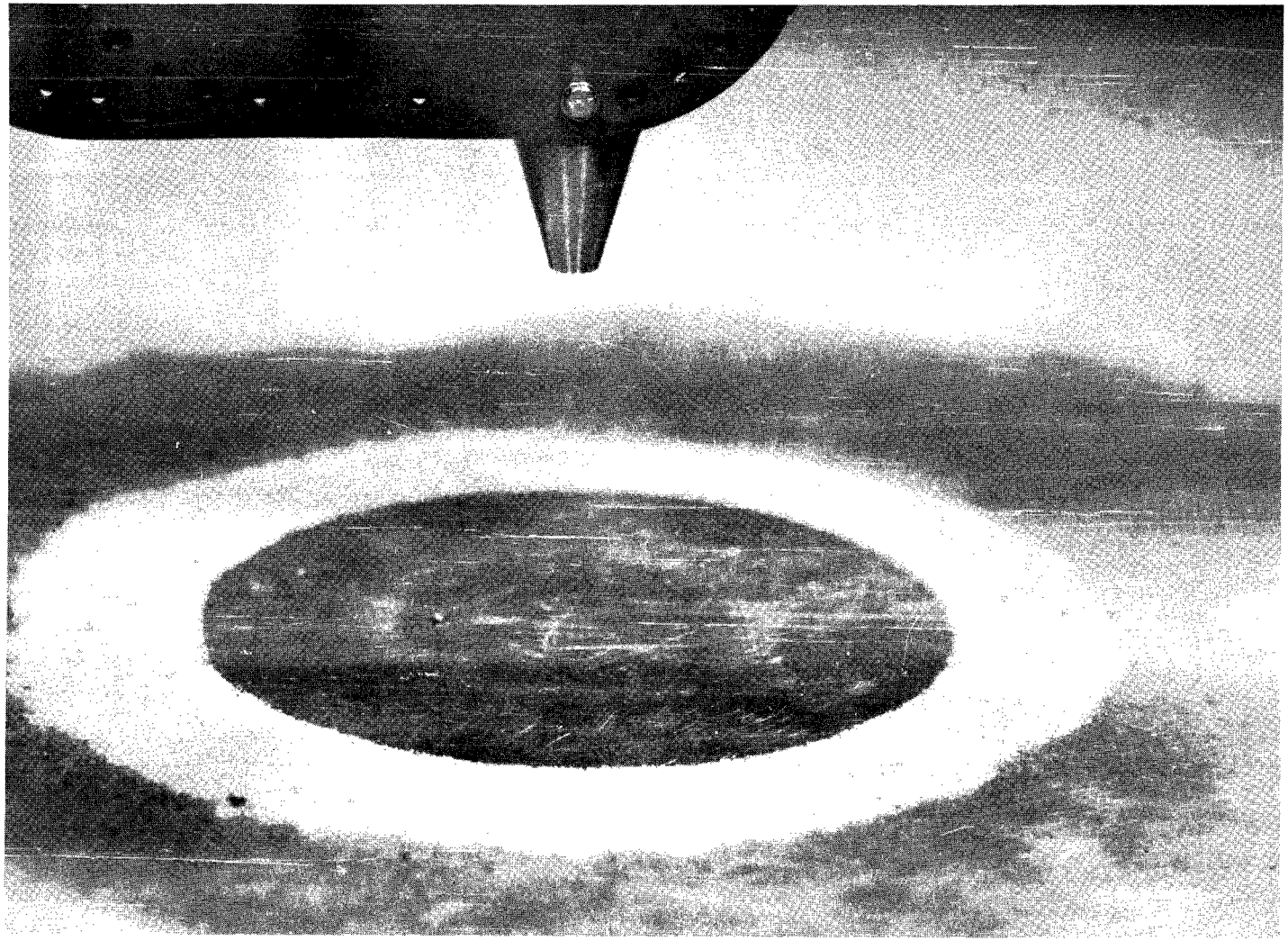

(d) t_o + 8.200 seconds. L-64-4795

Figure 16.- Continued.

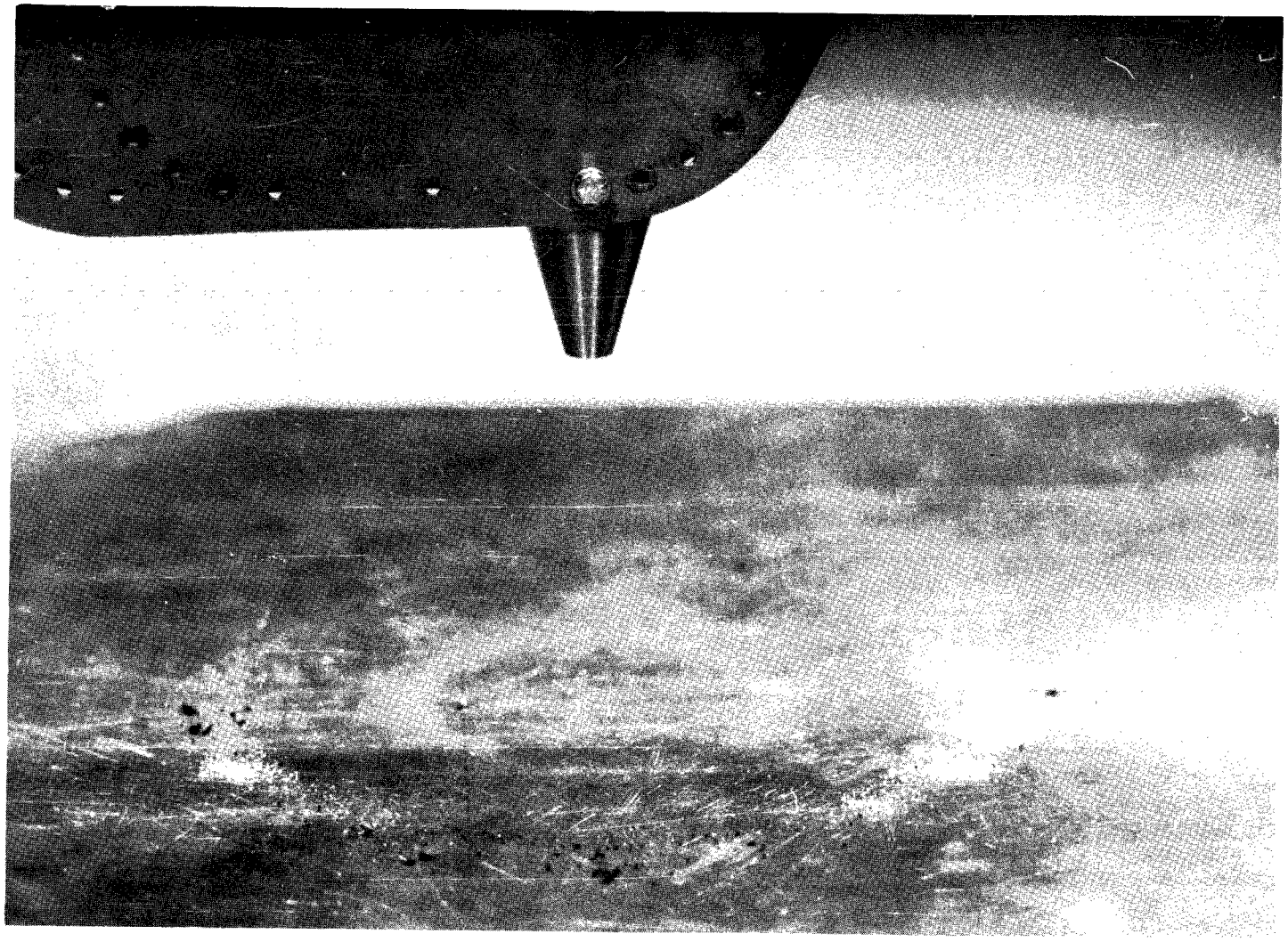

(e) t_o + 10.000 seconds.

L-64-4796

Figure 16.- Concluded.

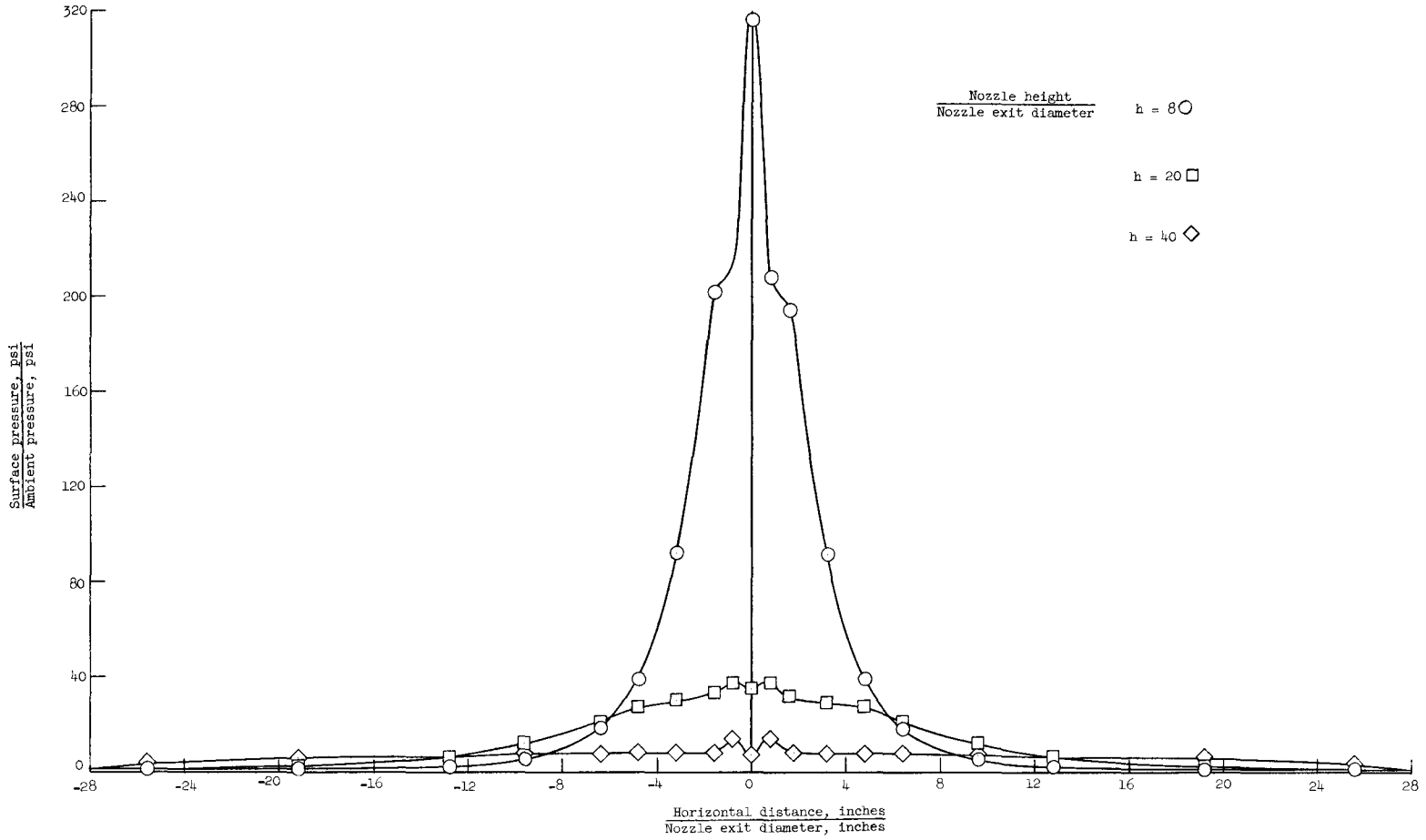

Figure 17.- Surface pressure measurements obtained from tests of single Mach 5 nozzle blasting on flat plate.

A motion-picture film supplement L-689 (two reels) is available on loan. Requests will be filled in the order received. You will be notified of the approximate date scheduled.

The film (16 mm, 38 min, black and white, silent) shows two Mach 5 nozzles which were used to simulate the rocket engines of a space vehicle which would be capable of making a vertical lunar descent and landing.

Requests for the film should be addressed to:

Chief, Photographic Division
NASA Langley Research Center
Langley Station
Hampton, Va. 23365

C U T

Date _____

Please send, on loan, copy of film supplement L-689 (two reels) to TN D-2455

_____
Name of organization

_____
Street number

_____
City and State Zip code

Attention: Mr. _____

Title _____

"The aeronautical and space activities of the United States shall be conducted so as to contribute . . . to the expansion of human knowledge of phenomena in the atmosphere and space. The Administration shall provide for the widest practicable and appropriate dissemination of information concerning its activities and the results thereof."

—NATIONAL AERONAUTICS AND SPACE ACT OF 1958

NASA SCIENTIFIC AND TECHNICAL PUBLICATIONS

TECHNICAL REPORTS: Scientific and technical information considered important, complete, and a lasting contribution to existing knowledge.

TECHNICAL NOTES: Information less broad in scope but nevertheless of importance as a contribution to existing knowledge.

TECHNICAL MEMORANDUMS: Information receiving limited distribution because of preliminary data, security classification, or other reasons.

CONTRACTOR REPORTS: Technical information generated in connection with a NASA contract or grant and released under NASA auspices.

TECHNICAL TRANSLATIONS: Information published in a foreign language considered to merit NASA distribution in English.

TECHNICAL REPRINTS: Information derived from NASA activities and initially published in the form of journal articles.

SPECIAL PUBLICATIONS: Information derived from or of value to NASA activities but not necessarily reporting the results of individual NASA-programmed scientific efforts. Publications include conference proceedings, monographs, data compilations, handbooks, sourcebooks, and special bibliographies.

Details on the availability of these publications may be obtained from:

SCIENTIFIC AND TECHNICAL INFORMATION DIVISION

NATIONAL AERONAUTICS AND SPACE ADMINISTRATION

Washington, D.C. 20546